ACADEMIC PRESS

Available online at www.sciencedirect.com
SCIENCE DIRECT®

Journal of Catalysis 216 (2003) 487–504

JOURNAL OF CATALYSIS

www.elsevier.com/locate/jcat

The double-layer approach to promotion, electrocatalysis, electrochemical promotion, and metal–support interactions

C.G. Vayenas,* S. Brosda, and C. Pliangos

Department of Chemical Engineering, 1, Caratheodory St., University of Patras, GR-26500 Patras, Greece

Received 8 July 2002; revised 24 August 2002; accepted 13 September 2002

Abstract

Recent progress in understanding and modeling promotion, electrocatalysis, electrochemical promotion, and metal–support interactions is surveyed. It is shown that via the action of spillover and via the concept of the sacrificial promoter, the phenomena of promotion, electrochemical promotion, and metal–support interactions are functionally identical and only operationally different, as they all correspond to catalysis in presence of a controllable double layer. This is then utilized to derive adsorption isotherms and kinetic expressions which account explicitly for the electrostatic interactions between the double layer and the adsorbed reactants, intermediates, and products. The resulting analytical expressions are shown to be in excellent semiquantitative agreement with experiment and with the recently established promotional rules.

1. Introduction

1.1. Catalytic and electrocatalytic kinetics

Heterogeneous catalysis and aqueous or solid electrochemistry have been treated traditionally as different branches of physical chemistry, and yet similar concepts are used to model their kinetics [1–4] and similar surface science techniques are used to investigate their fundamental aspects at the molecular level [1–8]. The growing technological interest in fuel cells, both high-temperature solid oxide fuel cells (SOFC) and low-temperature polymeric electrolyte membrane (PEM) fuel cells, has brought the catalytic and electrochemical communities closer, as the merits of catalysis in designing and operating efficient anodes and cathodes is being more widely recognized [9–11].

An important additional operating parameter in electrochemical (electrocatalytic, i.e., net charge transfer) vs catalytic (no net charge transfer) kinetics is the electrical potential dependence of the electrochemical rate, yet in recent years its has been shown that for electrochemically promoted catalysts (i.e., catalysts in contact with a solid electrolyte [12–17]) the *catalytic* rate also depends dramatically on catalyst potential, similarly to the electrochemical rate.

1.2. Electrochemical promotion of catalysis

The idea of using an electronically conductive metal or metal oxide porous film simultaneously as a catalyst and as an electrode can be traced to the last works of Wagner [18]. This led not only to the passive technique of solid electrolyte potentiometry (SEP) for measuring in situ the chemical potential of oxygen on catalyst–electrodes [19], but, much more important, to the discovery of the effect of electrochemical promotion of catalysis (EPOC) or non-Faradaic electrochemical modification of catalytic activity (NEMCA effect [12–17,20–34]).

The basic phenomenology of this effect when using O^{2-}-, Na^{+}-, and H^{+}-conducting solid electrolytes is shown in Figs. 1–3. The (usually porous) metal catalyst–electrode, typically 2–5 μm thick, is deposited on the solid electrolyte and under an open circuit ($I = 0$, no electrochemical rate) produces a catalytic rate r_0 for, for example, C_2H_4 oxidation [35,36] (Figs. 1 and 3) or CO oxidation [37] (Fig. 2). Application of an electrical current, I, or potential (±2 V) between the catalyst and a counterelectrode causes very pronounced and non-Faradaic (i.e., $\Delta r \gg I/2F$) alterations to the catalytic rate, r, and, quite often, to the product

* Corresponding author.
E-mail address: cat@chemeng.upatras.gr (C.G. Vayenas).

0021-9517/03/$ – see front matter
doi:10.1016/S0021-9517(02)00127-6

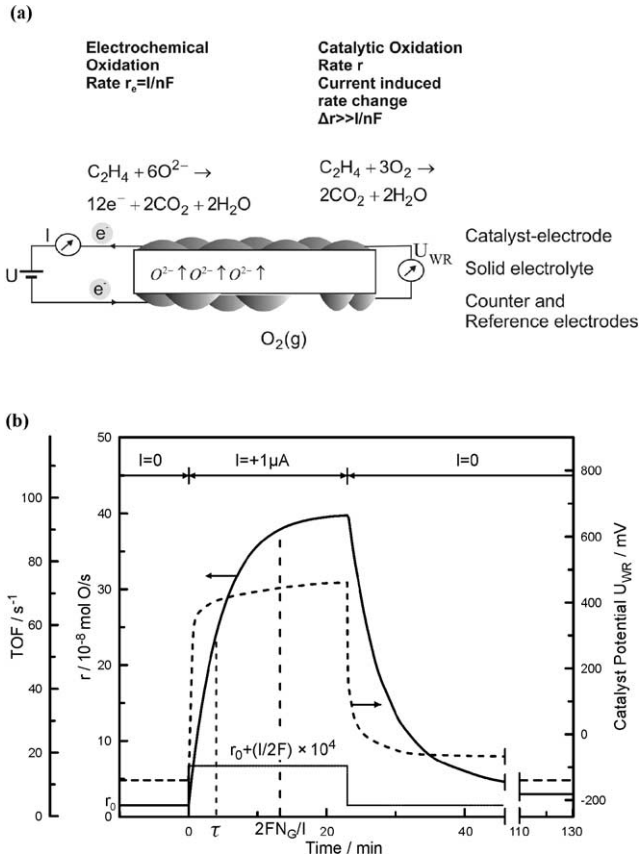

Fig. 1. (a) Basic experimental setup and operating principle of electrochemical promotion with O^{2-} conducting supports. (b) Catalytic rate, r, and turnover frequency, TOF, response of C_2H_4 oxidation on Pt deposited on YSZ, an O^{2-} conductor, on step changes in applied current [16,35]. $T = 370$ °C; $p_{O_2} = 4{,}6$ kPa; $p_{C_2H_4} = 0.36$ kPa. Also shown (dashed line) is the catalyst–electrode potential, U_{WR}, response with respect to the reference, R, electrode. The catalytic rate increase, Δr, is 25 time larger than the rate, r_0, before current application and 74,000 times larger than the rate, $I/2F$, of O^{2-} supply to the catalyst–electrode. N_G is the Pt/gas interface surface area, in mol Pt, and TOF is the catalytic turnover frequency (mol O reacting per surface Pt mol per s). Reprinted with permission from Kluwer/Plenum Publishers [16].

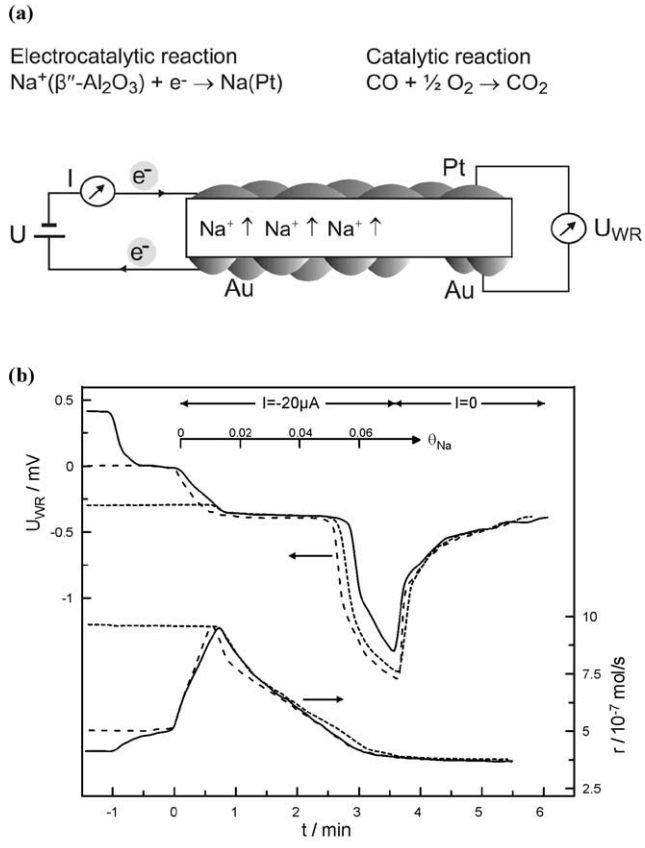

Fig. 2. (a) Basic experimental setup and operating principle of electrochemical promotion with Na^+ conducting supports. (b) Catalytic rate, r, response of CO oxidation on Pt deposited on β''-Al_2O_3, a Na^+ conductor, on step changes in applied current [37]. Also shown is catalyst potential, U_{WR}, response. $T = 350$ °C; $p_{CO} = 2$ kPa; $p_{O_2} = 2$ kPa. Note that the rate passes through a maximum at $\theta_{Na} = 0.015$, as the reaction rate of CO oxidation on Pt exhibits volcano-type behaviour with respect to the catalyst potential and work function [37]. On current interruption ($I = 0$) the rate, r, and potential, U_{WR}, do not return to their initial values. This is accomplished only by imposing potentiostatically the initial U_{WR} value [37]. In this experiment the potentiostat, previously used to control U_{WR}, is disconnected at $t = -1$ min and then at $t = 0$ the galvanostat is used to apply a constant current [37]. Dashed curves correspond to rate and U_{WR} transients obtained with different previously imposed U_{WR} values. Note that the Na coverage (inset axis) always determines the r and U_{WR} values during the transients [37].

selectivity, e.g., Fig. 4 [15,16,29]. The rate of the catalytic reaction, r, can become up to 200 times larger than the open-circuit rate, r_0, and up to 3×10^5 times larger than the Faradaic rate ($I/2F$ for O^{2-}, $-I/F$ for Na^+ and H^+) of ion supply (or removal) to (or from) the catalyst–electrode [15, 16]. The Faradaic efficiency, Λ, defined as

$$\Lambda \equiv \Delta r(\text{catalytic}) \big/ (I/nF), \tag{1}$$

where n is the ion charge, can thus reach values of up to 3×10^5 or down to -10^4 [15,16]. Electrocatalysis is limited to $|\Lambda| \leqslant 1$, and this is the main distinguishing feature of electrocatalysis and electrochemical promotion.

Up to 2001 [16], more than 70 different catalytic reactions (oxidations, hydrogenations, dehydrogenations, isomerizations, decompositions) have been electrochemically promoted on Pt, Pd, Rh, Ag, Au, Ni, IrO_2, and RuO_2 catalysts deposited on O^{2-} (YSZ), Na^+ (β''-Al_2O_3), H^+ ($CaZr_{0.9}In_{0.1}O_{3-\alpha}$, Nafion), F^- (CaF_2), aqueous [33,38], molten salt [31], and mixed ionic–electronic (TiO_2 [39], CeO_2 [40]) conductors.

Clearly EPOC is not limited to any particular class of conductive catalyst, catalytic reaction, or ionic support. The first commercial electrochemically promoted soot combustion units have been recently produced by Dinex in Denmark [16,41].

1.3. Basic questions

After it became apparent in the early 1990s [42] that electrochemical promotion is a general effect at the interface of

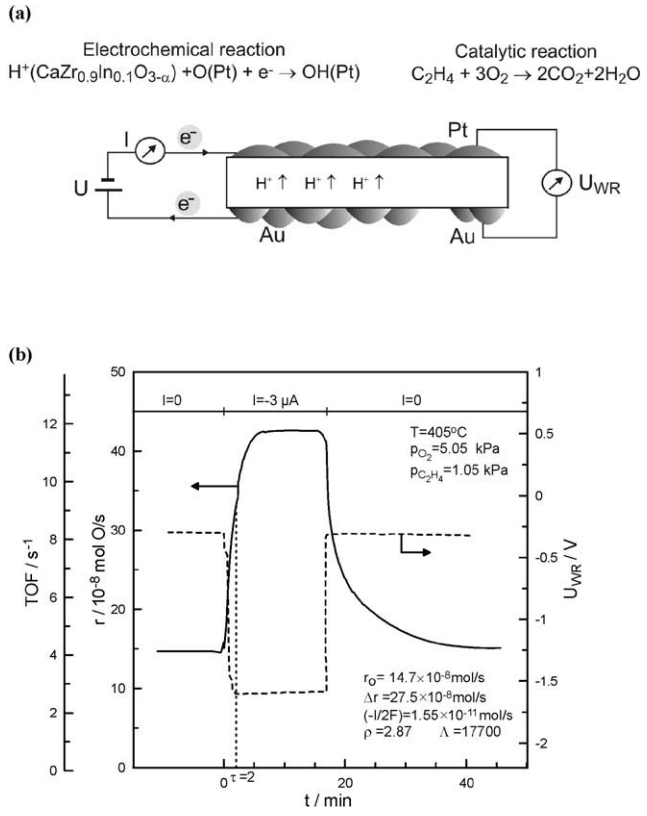

Fig. 3. (a) Basic experimental setup and operating principle of electrochemical promotion using a H^+ conductor during C_2H_4 oxidation on Pt deposited on $CaZr_{0.9}In_{0.1}O_{3-\alpha}$ [36]. (b) Catalytic rate, r, catalytic turnover frequency, TOF, and catalyst potential response to step changes in applied current. The increase in O consumption, Δr, is 17,700 times larger than that anticipated from Faraday's law and corresponding rate, $-I/F$, of proton transfer to the Pt catalyst.

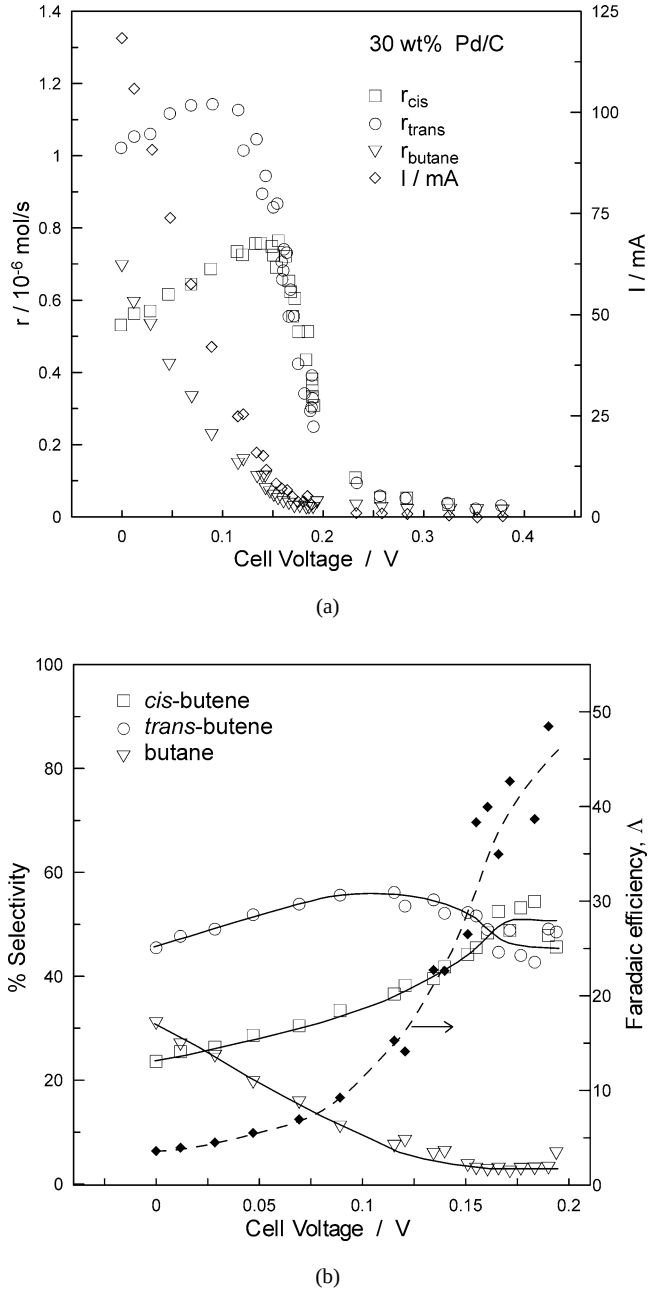

Fig. 4. (a) Electrochemical promotion of an isomerization reaction [29]. Steady-state effect of cell potential on the cell current, I, and on the rates of formation of *cis*-2-butene, *trans*-2-butene, and butane produced from 1-butene supplied over a dispersed Pd/C catalyst–electrode deposited on Nafion, a H^+ conductor, at room temperature [29]. Reprinted with permission from the American Chemical Society. (b) Corresponding effect of cell potential on the selectivities to *cis*-2-butene, *trans*-2-butene, and butane and on the apparent Faradaic efficiency, Λ, defined as $\Delta r_{\text{total}}/(I/F)$. Thus, each proton catalyzes the isomerization of roughly 50 molecules of 1-butene to *cis*-and *trans*-2-butene [29].

catalysis and electrochemistry, several important questions were raised, which can be summarized as follows: *What is the molecular origin of electrochemical promotion and how does it relate to*: (i) *Electrocatalysis*; (ii) *Classical* (*or chemical, conventional*) *promotion* (*where the promoter is added to the catalyst ex situ, i.e., during catalyst preparation*); *and* (iii) *Metal–support interactions*?

The last part of the question became relevant because of the following two discoveries.

(a) Mixed electronic–ionic conducting supports, such as TiO_2 [39] or CeO_2 [40], can replace YSZ in inducing NEMCA, a very noteworthy observation in view of the fact that TiO_2 and CeO_2 are relatively common conventional catalyst supports, and their ionic conductivity is, at best, only 3% of their electronic *n*-type conductivity [39,40].

(b) Just short-circuiting the catalyst and counterelectrode and taking advantage of the potential difference spontaneously generated, under an open circuit, between the catalyst and counterelectrode, due to their different activity for the catalytic reaction, just as in the case of single-chamber fuel cells [43], is sufficient to induce NEMCA at least for electrophobic reactions, i.e., catalytic reactions where the rate increases with increasing potential, or with O^{2-} supply to the catalyst (Fig. 5a). This key experiment of Cavalca et al. [26] was the first "wireless" or, more precisely, "self-

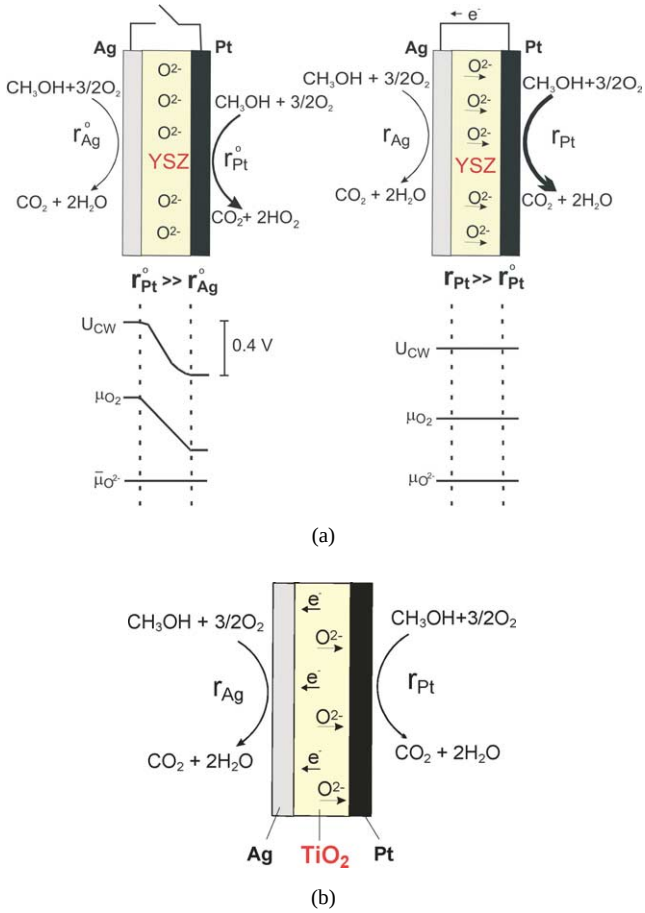

Fig. 5. (a) Self-driven electrochemical promotion of a Pt catalyst for CH_3OH oxidation to CO_2, an electrophobic reaction [26] observed on short-circuiting ($U_{CW} = 0$) the Pt catalyst–electrode with the Ag counterelectrode deposited on YSZ at 380 °C [26]. See text for discussion. (b) Principle of self-driven electrochemical promotion of the same catalytic reaction on a Pt catalyst deposited on a mixed electronic–ionic conductor such as TiO_2 [16]. The Pt catalyst and Ag counterelectrode are internally short-circuited via the electronic conduction of the support.

driven" NEMCA experiment. It showed the following:

(i) That a power source (galvanostat or potentiostat) is not necessary to induce NEMCA.
(ii) That if the support has both electronic and ionic conductivity (e.g., TiO_2), then NEMCA is induced even without external (via a wire) short-circuiting of the catalyst and counterelectrode. The short-circuiting is internal (Fig. 5b) and the Pt/TiO_2 catalyst is electrochemically promoted without any wire attached to it, giving thus macroscopically all the symptoms of a metal–support interaction.

2. Origin of electrochemical promotion

It took several years and the use of a heavy arsenal of (i) surface science techniques, including XPS [16,24,44–46], UPS [46], TPD [47–50] (Fig. 6), PEEM [51], and STM [52,53] (Fig. 7), (ii) more conventional catalytic techniques, including rate transient analysis [16] and work-function measurements [14,16,53], (iii) electrochemical techniques, including cyclic voltammetry [16,47] (Fig. 6) and AC impedance spectroscopy [54,55], and (iv) theoretical ab initio quantum mechanical calculations [56,57] to fully understand the origin of electrochemical promotion. All these techniques have provided a unanimous answer to the problem:

> *Electrochemical promotion is due to the current or potential-controlled electrocatalytic* (*Faradaic*) *introduction of promoting species* (*e.g.*, $O^{\delta-}$, $Na^{\delta+}$) *from the solid electrolyte to the catalyst/gas interface where an overall neutral double layer is formed. The density of this double layer* (*and the field strength in it*) *varies as the applied potential is varied and this affects both the work function of the surface and the chemisorptive bond strength of reactants and intermediates, thus causing dramatic and reversible alterations in catalytic rate* (Fig. 8).

In case the promoting species can also participate in the catalytic reaction (e.g., $O^{\delta-}$ originating from YSZ [45] or TiO_2 [39], which is quite distinct from chemisorbed oxygen originating from gas phase O_2), it acts as a *sacrificial* promoter, i.e., it promotes the catalytic reaction (via repulsive or attractive lateral interactions), but it also gets consumed at a rate which is Λ times smaller than the rate of consumption of the catalytic reactant, e.g., atomic O originating from the gas phase [16] (Fig. 9). The concept of the *sacrificial promoter*, also discussed below, is the key to understanding electrochemical promotion with O^{2-} conductors.

This molecular mechanism is unanimously supported by all the above surface science, catalytic, and electrochemical techniques. A combination of the results of any two or three of them would have sufficed to put together the puzzle. But each of them had something new to offer, some new facet of the surface chemistry to reveal. As Pritchard correctly predicted in his 1990 *Nature* editorial on NEMCA [58]:

> *"The strong long-range effect implied by the correlation of work-function change with activation-energy change found by Vayenas et al.* [14] *in the presence of electrochemically induced promotion is particularly intriguing. So too is the nature of the electrochemically induced oxygen species that is believed to cause the increase in work function and catalytic promotion, yet which is less reactive than the adsorbed oxygen reactant that covers most of the surface. There is clearly much surface chemistry to be explored and it will be interesting to see how general the work-function effect proves to be. In any case, the ability to vary the concentration of promoters by electrochemical control while under reaction conditions is a valuable development in catalytic research, and one can expect it to be rapidly exploited in conjunction with other in situ techniques of surface analysis."*

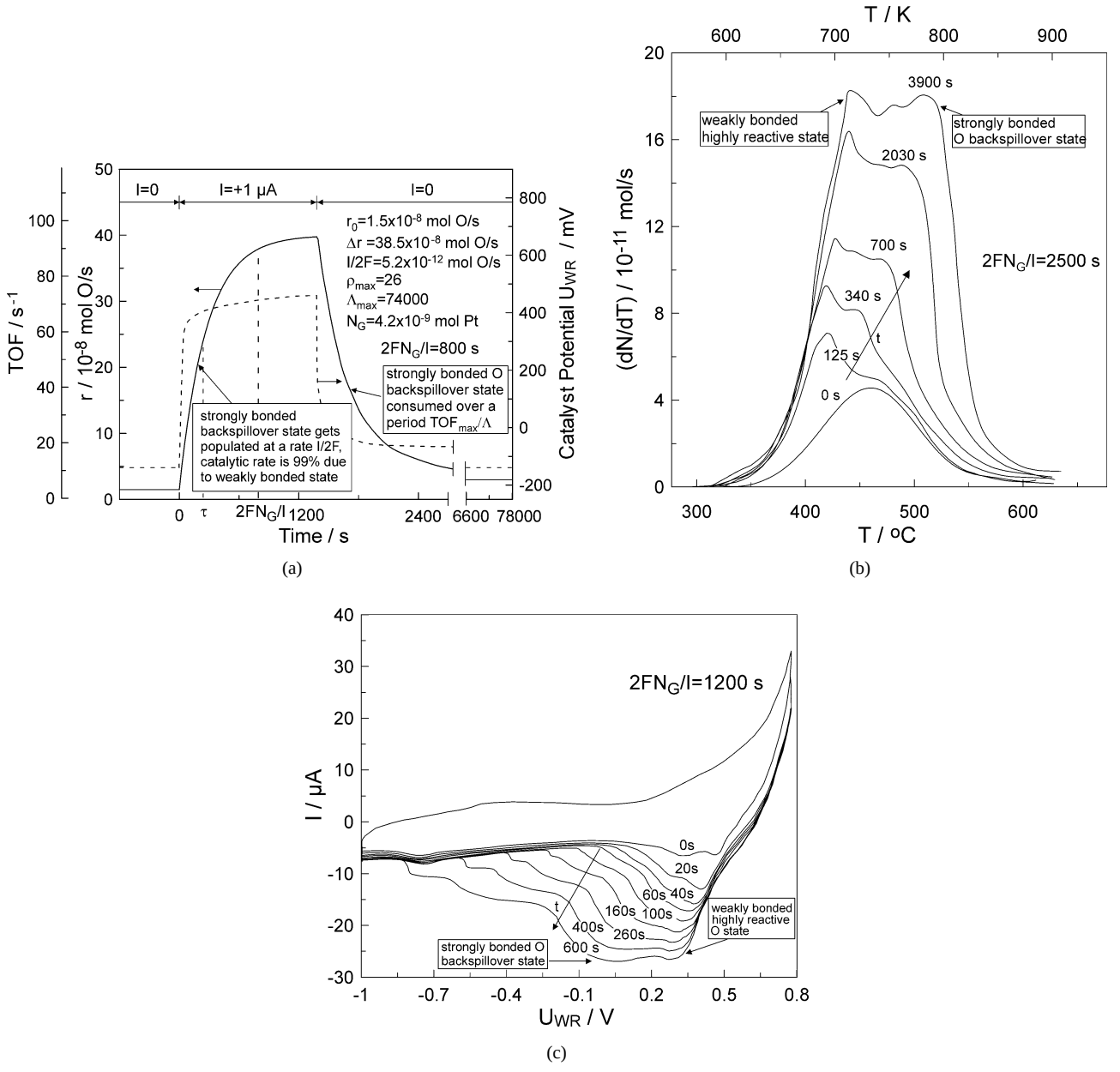

Fig. 6. NEMCA and its origin on Pt/YSZ catalyst electrodes [16]. Transient effect of the application of a constant current (a, b) or constant potential U_{WR} (c) on (a) the rate, r, of C_2H_4 oxidation on Pt/YSZ (also showing the corresponding U_{WR} transient), (b) the O_2 TPD spectrum on Pt/YSZ after current ($I = 15$ μA) application for various times t. (c) The cyclic voltammogram of Pt/YSZ after holding the potential at $U_{WR} = 0.8$ V for various times t. Reprinted with permission from Kluwer/Plenum Publishers [16].

Twelve years and hundreds of publications later [16], one might only wish to change "that is believed to cause" into "which causes" in the above eloquent, concise, and almost prophetic description of the origin of electrochemical promotion.

Several questions, of course, still remain open, such as the exact nature of the "permanent NEMCA" effect discovered by Comninellis and co-workers [59], which could have important applications in the scientific preparation of supported catalysts [60,61], but the basic phenomenology of NEMCA is today not only well understood, it is to a large extent quite predictable [16].

3. Promotion, electrochemical promotion, and metal–support interactions

3.1. New problems

As is often the case in the natural sciences the quest of solving one problem (origin of electrochemical promotion) quite often leads to the definition and solution of other problems which at a first glance look unrelated. In this respect the quest is frequently more important than the original problem solution itself, and this has been the case with electrochemical promotion as well. So here we list,

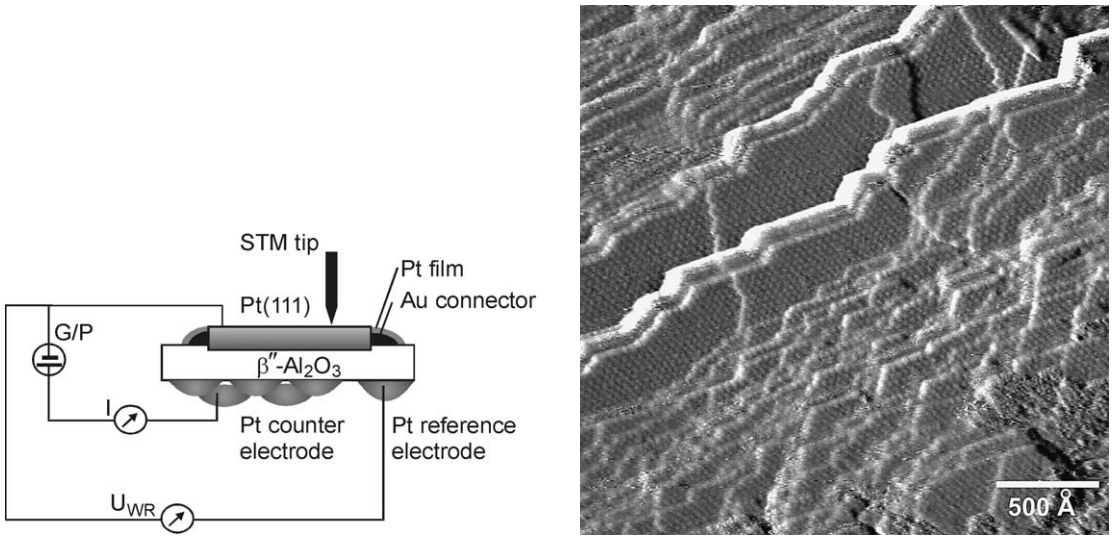

(a) (c)

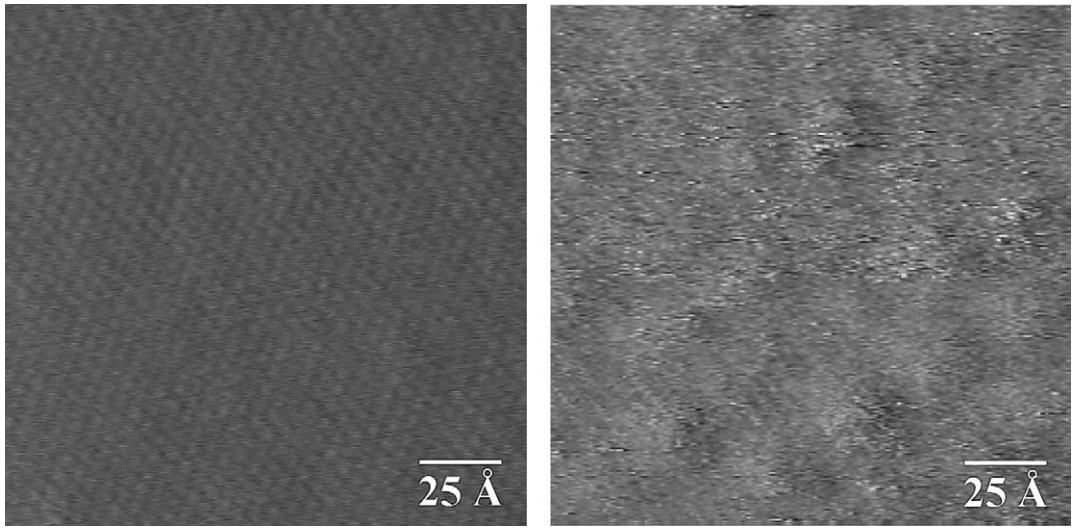

(b)

Fig. 7. (a) Schematic of the experimental setup for using STM to investigate the Pt(111) surface of a Pt single crystal interfaced with β''-Al_2O_3. (b) Low-scanning-area STM images (unfiltered) of the (left) sodium-cleaned and (right) sodium-dosed Pt(111)–(2×2)-O adlattice. Total scan size, 159 Å [52]. Reprinted with permission from Elsevier Science. (c) Larger scanning area STM image (unfiltered) of a Pt single-crystal surface consisting mainly of Pt(111) terraces and covered by a Pt(111)–(12×12)-Na adlattice formed via an electrochemical Na^+ supply on the Pt(111)–(2×2)-O adlattice. Each sphere on the image corresponds to a Na atom [53]. Reprinted with permission from the Electrochemical Society.

in increasing order of importance and *apparent* irrelevance, four major problems in heterogeneous catalysis and then proceed to discuss the insight gained for their solution, as it has emerged in the last 5 years as a by-product of the quest of the origin of electrochemical promotion.

1. The relationship between electrochemical and classical (chemical or conventional) promotion [62,63].
2. The molecular mechanism of metal–support interactions [64–70] and their effect on chemisorption and catalysis.
3. The reason for gradual substitution during the last few years of classical industrial supports (SiO_2, γ-Al_2O_3) with mixed conducting electronic–ionic supports based on ZrO_2, Y_2O_3, TiO_2, and CeO_2 in many areas of practical catalysis [71–77] and particularly in oxidation catalysis [70].
4. Prediction of the type of support and type of promoter needed for each catalyst and catalytic reaction [78].

3.2. Functional equivalence of electrochemical and classical promotion: spillover and the concept of a sacrificial promoter

Since the early days of electrochemical promotion of catalysis (EPOC) in the 1980s [35], it became clear via galvanostatic (constant current) catalytic rate transients,

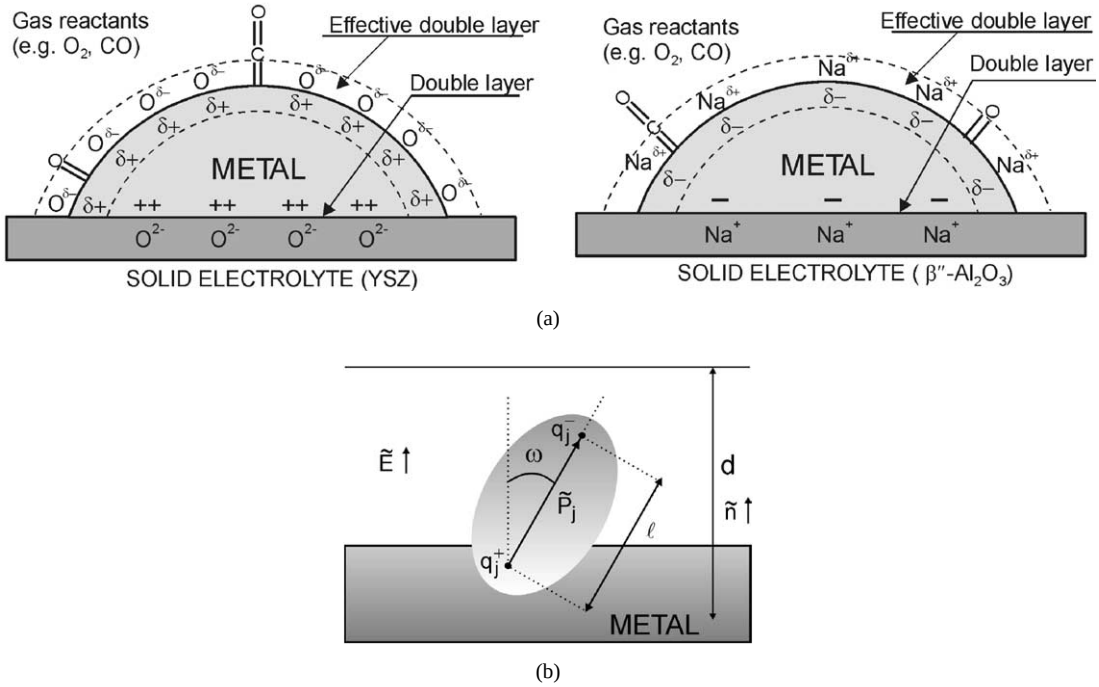

Fig. 8. (a) Schematic representation of a metal electrode deposited on a O^{2-}-conducting (left) and on a Na^{+}-conducting (right) solid electrolyte, showing the location of the metal–electrolyte double layer and of the effective double layer created at the metal/gas interface due to potential-controlled ion migration (backspillover). (b) Schematic of an adsorbate, modeled as a dipole, in the presence of the double layer at the metal/gas interface [16]. Reprinted with permission from Kluwer/Plenum publishers.

such as those shown in Figs. 1–3, that EPOC is due to current or potential-controlled migration of a promoting species from the support to the catalyst (the term backspillover or reverse spillover has been used traditionally to denote such a migration from the support to the catalyst and we also use it here, as opposed to spillover, which usually denotes migration in the opposite direction). The fact that the time needed for the catalytic rate to reach its new electrochemically promoted state is always on the order of $2FN_G/I$ (Fig. 1), where N_G is the catalyst/gas interface surface area expressed in moles of metal and I is the applied constant current, provided strong evidence for this, since $2FN_G/I$ is the time required to form a monolayer of O^{2-} on a metal surface with N_G surface sites.

In the case of Na^{+}-conducting electrolyte supports, such as β''-Al_2O_3 [37], both adsorbed Na dipole moment measurements (3–10 D) [37,42] and the elegant XPS studies of Lambert and co-workers [17] showed clearly that electrochemically introduced $Na^{\delta+}$ is indistinguishable from gas-phase-supplied evaporated $Na^{\delta+}$ on the metal catalyst surface. Thus in this case the origin of EPOC was quite clear: Electrocatalytic (Faradaic) introduction of a classical promoter ($Na^{\delta+}$) on the catalyst surface (Figs. 7 and 8). The promoter can then affect the catalytic rate, r, in a manner which is not restricted by Faraday's law. Consequently, in this case, electrochemical and classical promotion are *functionally identical* and only operationally different. However, in the case of O^{2-}-conducting solid electrolytes (YSZ) or mixed ionic (O^{2-})–electronic conductors (TiO_2, CeO_2), this functional identity was not obvious, since the promoting species, O^{2-}, was unknown from classical promotion studies. Thus it took the intensive use of XPS [39,45], TPD [47–50], cyclic voltammetry [47], PEEM [50], and STM [15,16,52,53], together with the introduction of the concept of a *sacrificial promoter* [15], to elucidate the situation and prove the functional identity of promotion and electrochemical promotion.

The key for understanding electrochemical promotion with O^{2-} conductors is to realize that two oxygen species coexist on the metal catalyst surface, as evidenced, for example, by TPD or cyclic voltammetry (Fig. 6). One is normally chemisorbed atomic oxygen, O(a), originating from the gas phase

$$O_2(g) \rightarrow 2O(a). \tag{2}$$

The other oxygen species is the promoting anionic species which migrates (backspillovers) from the solid electrolyte, i.e.,

$$O^{2-}(YSZ) \rightarrow \left[O^{\delta-}, \delta+\right] + 2e^{-}, \tag{3}$$

where the symbol $[O^{\delta-}, \delta+]$ is used to underscore the fact that $O^{\delta-}$ is accompanied by its compensating charge δ^{+} in the metal and thus forms an overall neutral dipole (as the normally chemisorbed oxygen O(a) also does, but with a significantly smaller dipole moment [49,50]). There is strong evidence from XPS [16] that $\delta = 2$ and thus $O^{\delta-}$ is O^{2-}, but to stay on the conservative side, we still use $O^{\delta-}$.

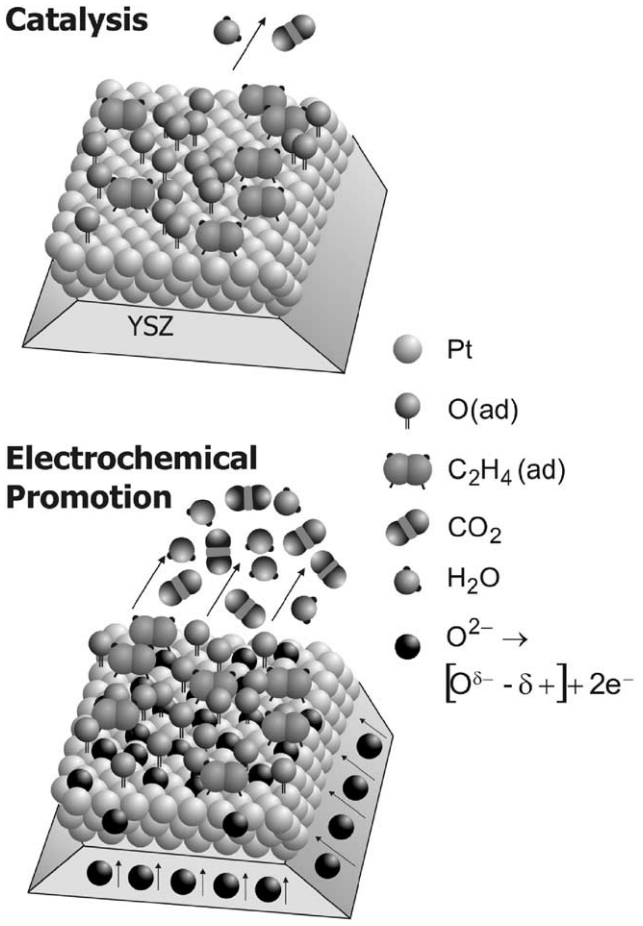

Fig. 9. Atomic visualization of NEMCA during ethylene C_2H_4 on Pt/YSZ. The backspillover $[O^{\delta-}\text{-}\delta+]$ species forces O(ad) to a more weakly bound and more reactive state [16]. Reprinted with permission from Kluwer/Plenum publishers.

The promoting anionic $O^{\delta-}$ species is more strongly bonded then O(a) on the surface [47–50] and is significantly less reactive than O(a) in oxidation reactions [15,16,47–50].

We denote by r and r_p the rates of consumption of the two oxygen species with the oxidizable reactant (e.g., C_2H_4; Fig. 1) and by TOF and TOF_p the corresponding turnover frequencies (in terms of the total Pt atoms present on the surface). We also denote by τ and τ_p the corresponding average lifetimes of O(a) and $[O^{\delta-}, \delta^+]$ on the catalyst surface. One can easily show that, for sufficiently large Faradaic efficiency Λ values, it is

$$\Lambda = \frac{r}{r_p} = \frac{\mathrm{TOF}}{\mathrm{TOF}_p} = \frac{\tau_p}{\tau}. \tag{4}$$

Thus for a fast electrochemically promoted reaction, e.g., C_2H_4 oxidation (Fig. 1), it is TOF $\approx 10^2$ s^{-1}, $\tau = 10^{-2}$ s, $TOF_p = 10^{-3}$ s^{-1}, $\tau_p \approx 10^3$ s. The fact that τ_p is on the order on 10^3 s is also manifested in Fig. 1 by the fact that on current interruption, it takes approximately 10^3 s for the catalytic rate to return to its initial unpromoted value. In fact using the rate transient on current interruption to estimate τ_p and knowing τ (from the measured TOF) it is possible to use Eq. (4) and estimate Λ without knowing the value of the applied current I! This clearly demonstrates the validity of the *sacrificial promoter* concept.

The reason that $[O^{\delta-}, \delta^+]$, a most effective anionic promoter [15,16], was unknown from classical promotional studies is threefold. First, it does not form via gaseous O_2 adsorption. Second, in any spectroscopic investigation of an oxide-supported catalyst, its signal is masked by the O^{2-} signal of the support. Third, its short lifetime on the catalyst surface (typically 10–10^3 s) makes it useless for any practical promotional application, unless it is continuously replenished via contact with an O^{2-}-conducting solid electrolyte, as in electrochemical promotion experiments.

It is thus not accidental that $O^{\delta-}$ (most likely O^{2-}), the sacrificial promoter responsible for NEMCA with O^{2-} conductors, was first discovered via XPS [44,45] and, very recently, STM [79] on large ($\sim$ 1 cm) polycrystalline or single-crystal Pt(111) samples interfaced with YSZ and TiO_2. These studies have clearly established the functional identity of promotion and electrochemical promotion when using O^{2-} conductors.

So far there have been no surface spectroscopic investigations of EPOC using proton conductors. Since, however, the macroscopic phenomenology is identical to that of O^{2-} conductors (Fig. 3), it is very likely that the EPOC mechanism also in this case involves formation of a protonated sacrificial promoter, OH(a), on the catalyst surface; i.e.,

$$H^+ + O(a) + e^- \rightarrow OH(a), \tag{5}$$

where, again, the ratio of the surface lifetimes of OH(a) and O(a) determines the Faradaic efficiency, Λ, for oxidation reactions.

3.3. Mechanism of metal–support interactions

Metal–support interactions play an important role in the performance of many industrial supported catalysts. Since the time of Schwab [64], understanding the mechanism of metal–support interactions has been one of the central and most challenging problems in heterogeneous catalysis. The effect can be quite pronounced, as shown in Fig. 10 for the case of C_2H_4 oxidation on Rh dispersed on four different supports of increasing work function [80]. The sharp rate transition is due to surface Rh oxide formation, which poisons the oxidation rate [80,81]. The same figure shows one of the key experiments which proved the mechanistic equivalence of electrochemical promotion and metal–support interactions [80]. The r vs p_{O2} behavior obtained on the finely dispersed Rh catalyst on the four supports can be reproduced by varying the potential (and thus work function [14]) of a polycrystalline Rh film deposited on YSZ (Fig. 10, inset). Thus one can assign to each support an equivalent potential (Fig. 11a) which correlates linearly and with a slope of unity to the independently measured absolute potential [53] or work function [80] of the supports (Fig. 11b).

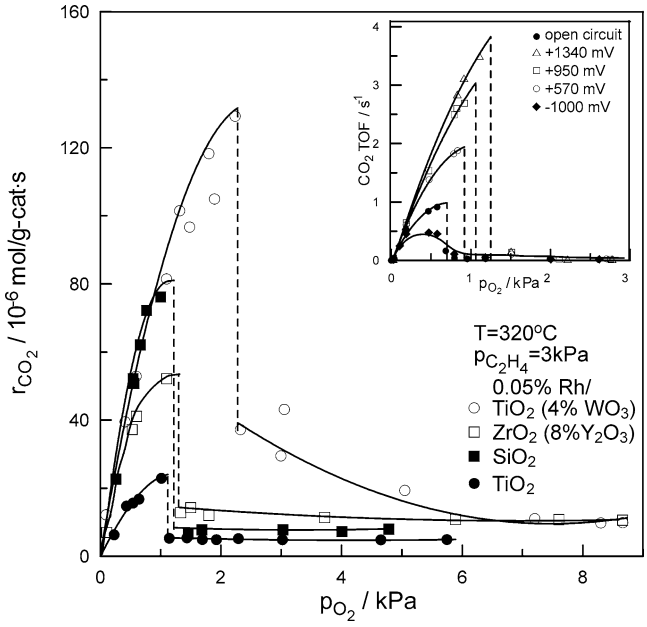

Fig. 10. Effect of p_{O_2} on the rate of C_2H_4 oxidation on Rh supported on four supports of increasing Φ. Catalyst loading, 0.5 wt% [80,81]. (Inset) Electrochemical promotion of a Rh catalyst film deposited on YSZ. Effect of potentiostatically imposed catalyst potential U_{WR} on the rate and TOF dependence on p_{O_2} at fixed $p_{C_2H_4}$ [80,81].

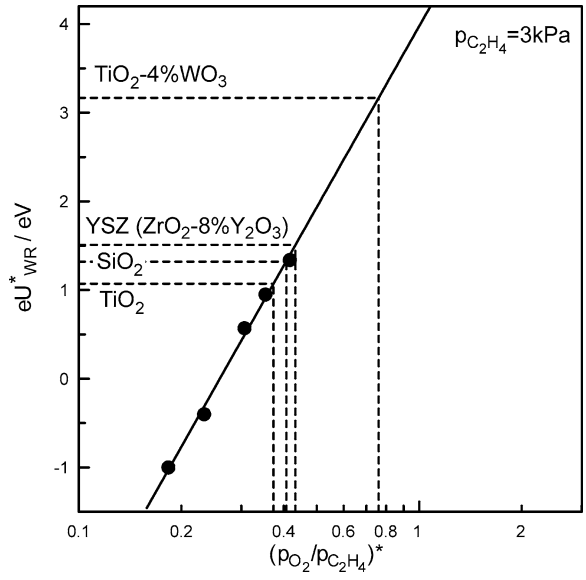

(a)

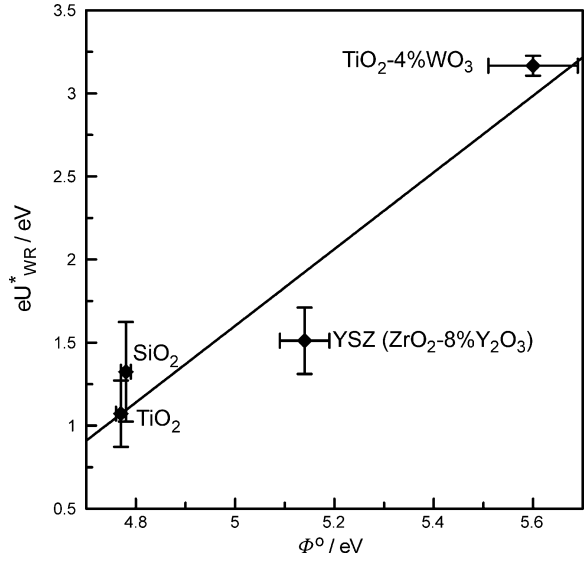

(b)

Fig. 11. (a) Effect of $(p_{O_2}/p_{C_2H_4})^*$ ratio at rate transition on the potential U^*_{WR} where the rate transition occurs during C_2H_4 oxidation on Rh films deposited on YSZ (Fig. 10 inset, circles) and on the equivalent potential U^*_{WR} where the same rate break occurs on different supports (Fig. 10). (b) Correlation between the equivalent potentials of the supports defined in (a) and of the work function or absolute potential [53,80] of the supports measured via the Kelvin probe technique in $p_{O_2} = 1$ atm at 400 °C [53,80].

Supports with higher absolute potential [53] or work function [53,80] have enhanced propensity for O^{2-} backspillover on the catalyst surface; therefore they enhance C_2H_4 oxidation, which is an electrophobic reaction, i.e., a reaction where the rate increases with increasing potential and work function (Fig. 10, inset).

Another key experiment which has shown the equivalence of electrochemical promotion and metal support interactions is shown in Fig. 12: IrO_2, a metallic oxide, and TiO_2 exhibit a strong metal–support interaction, as shown by the volcanotype rate dependence of C_2H_4 oxidation on catalyst composition [80,82].

As shown in an ingenious experiment by Nicole [82], pure IrO_2 can be electrochemically promoted by a factor of eleven ($\rho = r/r_0 = 11$) (Fig. 12), but IrO_2–TiO_2 catalysts are only marginally affected by electrochemical promotion. This is because they are already in a self-driven electrochemically promoted state via contact with TiO_2 [80,82] (Fig. 12). These two experiments, together with the self-driven electrochemical promotion experiments of Cavalca et al. [26] (Fig. 5) have shown conclusively that *electrochemical promotion is an electrically controlled metal–support interaction* (Fig. 13) and that *metal–support interactions on ZrO_2-, CeO_2-, or TiO_2-based supports are induced by reverse spillover of oxygen anions from the carrier onto the surface of the metal crystallites.*

Thus the same mathematical models describing diffusion and consumption of the sacrificial $O^{\delta-}$ promoter on electrochemically promoted NEMCA catalysts are applicable for dispersed catalysts deposited on ZrO_2, CeO_2, and TiO_2 supports [83].

It is worth noting that the "classical" approach to interpreting metal–support interactions is based on the view of "electron-transfer" between the catalyst and the support [64,65]. It neglects the ionic conductivity and thus O^{2-}-donating capacity of ZrO_2-, CeO_2-, and TiO_2-based supports which pins the Fermi level of supported nanoparticles to that of the support [16,80]. Thus the "classical" approach focuses

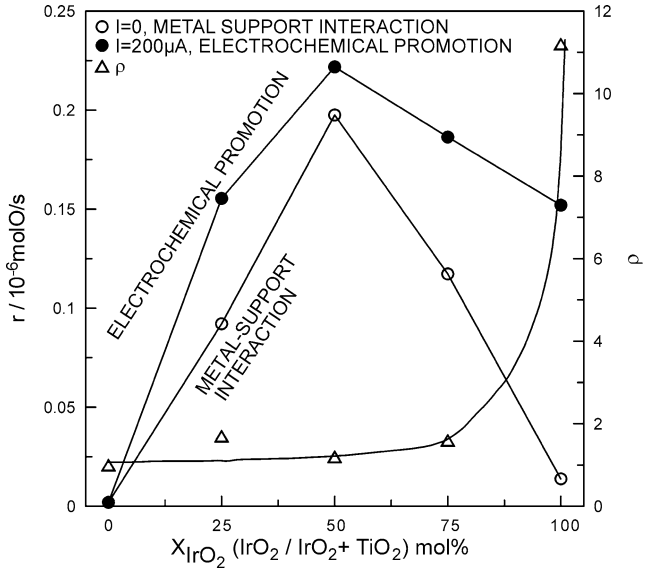

(a)

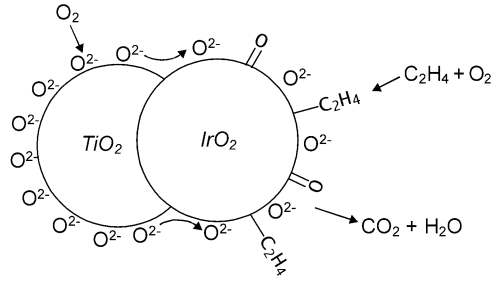

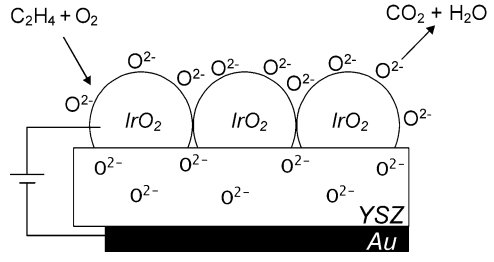

(b)

Fig. 12. (a) Effect of IrO_2 mol fraction in the IrO_2–TiO_2 catalyst [80,82] on the open-circuit catalytic rate, r_0, of C_2H_4 oxidation (○), on the electrochemically promoted ($I = 200$ μA) catalytic rate, r, (●), and on the corresponding rate enhancement ratio ρ (△). ($T = 380$ °C; $p_{O_2} = 20$ kPa; $p_{C_2H_4} = 0.15$ kPa). (b) Mechanism of metal (IrO_2)–support (TiO_2) interaction (top) during ethylene oxidation on IrO_2 and of electrochemical promotion utilizing YSZ (bottom) [80].

on the semiconductive and not the ionic properties of the support. The "electron transfer" view is correct, but only as the first step for inducing O^{2-} reverse spillover. Thus a support with high absolute potential or work function, such as YSZ ($\Phi_0 = 5.14$ eV), will initially receive some electrons from a supported metal of initially lower Φ, e.g., supported polycrystalline Rh, but the positive charge on Rh will induce O^{2-} reverse spillover to neutralize it [53]. The higher the work function and absolute potential of the support, the higher its ability to donate O^{2-} [80]. Consequently the "electrochemical promotion" view of metal–support interactions correctly predicts that the rate of electrophobic reactions, such as C_2H_4 oxidation (Fig. 10), increases with increasing work function of the support (Figs. 10 and 11), while the "electron transfer" approach leads to the opposite conclusion: Increasing support work function enhances the positive charge on the Rh nanoparticles; thus it enhances oxygen binding to the surface, which is the opposite of what Fig. 10 shows.

One may thus conclude that there is compelling evidence (Figs. 5, 10–12) for the metal–support interaction mechanism shown in Fig. 13.

3.4. Interrelation of promotion, electrochemical promotion, and metal–support interactions: the double-layer model of catalysis

Promotion, electrochemical promotion, and metal–support interactions are three, at first glance, independent phenomena which can affect catalyst activity and selectivity in a dramatic manner. We have already discussed the (functional) similarities and (operational) differences of promotion and electrochemical promotion. We have also discussed the functional similarities and only operational differences of electrochemical promotion and metal–support interactions on ionic and mixed conducting supports. It therefore follows that promotion, electrochemical promotion, and metal–support interactions on ion-conducting and mixed conducting supports are three different facets of the same phenomenon. They are all three linked via the phenomenon of spillover–backspillover *of the promoting species*. And they are all three due to the same underlying cause: the interaction of adsorbed reactants and intermediates with an effective double layer formed by promoting species at the metal/gas interface (Fig. 8).

For time scales shorter than that of a catalytic turnover (typically 10^{-2} to 10^2 s) the three phenomena are indistinguishable. Looking at the Na-promoted Pt surface in Fig. 7c and imagining that CO oxidation is taking place on that surface, it is not possible to distinguish whether this is a classically promoted surface where Na has been added from the gas phase or an electrochemically promoted one where Na originated from β''-Al_2O_3 interfaced with the Pt crystal, or whether it is the surface of a larger crystallite deposited on a porous β''-Al_2O_3 carrier where Na has spontaneously migrated on the Pt surface (metal–support interaction). The oxidation of CO (Fig. 2) will be equally promoted in all three cases.

Similar is the situation on a Pt surface decorated with O^{2-}, with the only difference being the experimental difficulty of introducing O^{2-} with classical promotion and its

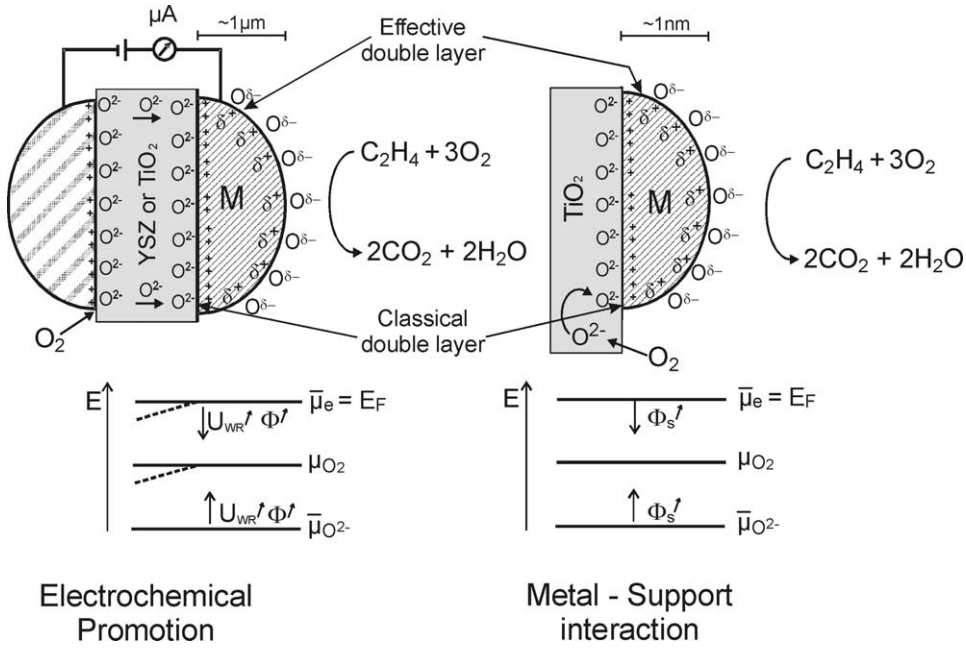

Fig. 13. Schematic of a metal grain (∼ μm) in a metal catalyst film deposited on YSZ or TiO_2 under electrochemical promotion conditions (left) and of a metal nanoparticle (∼ nm) deposited on a porous TiO_2 support (right) showing the locations of the classical double layers formed at the metal/support interface and of the effective double layers formed at the metal/gas interface. The energy diagrams (bottom) indicate schematically the spatial constancy of the Fermi level E_F (or electrochemical potential $\bar{\mu}_e$) of electrons, of the chemical potential of oxygen, and of the electrochemical potential of O^{2-}. Note that under electrical bias application (left) $\bar{\mu}_{O^{2-}}$ remains spatially constant but $\bar{\mu}_e$ and μ_{O_2} both bend in the solid electrolyte support (dashed lines). The Fermi level $\bar{\mu}_e$ of the metal can be affected by varying U_{WR} (left) or by varying via doping the Fermi level of the support (right) [16]. Reprinted with permission from Kluwer/Plenum publishers.

short lifetime on the catalyst surface, only Λ times longer than the catalytic turnover time.

Consequently the functional identity of classical promotion, electrochemical promotion, and metal–support interactions should not lead to pessimistic conclusions regarding the practical usefulness of electrochemical promotion. Operational differences exist between the three phenomena and it is very difficult to imagine how one can use metal–support interactions with conventional oxidic supports to promote an electrophilic reaction, or how one can use classical promotion to generate the strongest electronegative promoter, O^{2-}, on a catalyst surface. Furthermore there is no reason to expect that a metal–support-interaction-promoted catalyst is at its "best" electrochemically promoted state. Thus the experimental problem of inducing electrochemical promotion on fully dispersed catalysts remains an important one, as discussed in detail elsewhere [16].

Also important remains the issue of learning more, via surface spectroscopy, STM, and ab initio quantum chemical calculations, about the exact state and geometry of O^{2-} adsorption on metal surfaces. In the case, for example, of SMSI with TiO_2 catalysts, it is well documented [67] that the backspillover species is TiO_x, where x is a variable and about one for Pt. Although XPS investigations of Pt/YSZ [45,46] and Pt/TiO_2 [39] NEMCA catalysts have not so far provided evidence for any such anion/cation-pair electrochemically induced migration, this point is worth further investigation, particularly under reducing conditions. Regarding the adsorption geometry of O^{2-}, we have recently used STM to follow the migration of O^{2-} from YSZ onto Pt(111) under atmospheric pressure conditions [79], using the same design and procedure as in Fig. 7, but now with YSZ as the solid electrolyte. We found that under open-circuit conditions, most of the Pt(111) surface is covered by the well-known (2×2)-O adlattice, although patches of bare Pt(111) and patches of a (12×12)-O overlayer are also visible. After anodic polarization at 1 V, the Pt(111) surface and (2×2)-O adlattice are covered almost entirely by the (12×12)-O adlayer which corresponds to the electrochemically migrating O^{2-} species [79]. Each O^{2-} adspecies appears to be "large," i.e., it perturbs the electronic cloud of at least 10 neighboring O atoms of the coexisting (2×2)-O adlattice, which remains clearly visible [79]. These observations are consistent with the "long-range" promoting effect of O^{2-} and underscore the fact that, as Pritchard correctly predicted [58]," there is clearly much new surface chemistry to be explored."

Having discussed the functional similarity of classical promotion, electrochemical promotion, and metal–support interactions on O^{2-}-conducting and mixed electronic–ionic conducting supports, it is useful to also address and systematize their operational differences. This is attempted in Fig. 14: The main operational difference is the promoter lifetime, τ_p, on the catalyst surface.

For any practical classical promotion application in a fixed-bed catalytic reactor, τ_p must be longer than a year

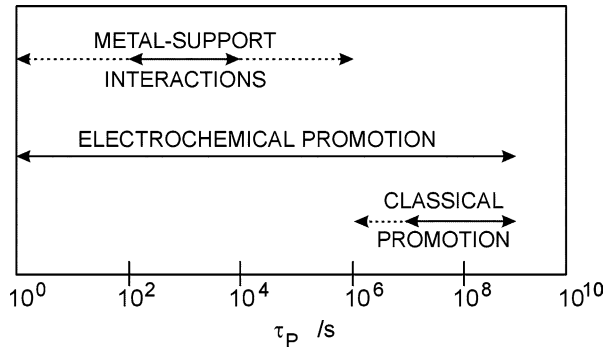

Fig. 14. Operational range of classical promotion, electrochemical promotion, and metal–support interactions in terms of the promoter lifetime, τ_p, on the catalyst surface [16].

($\sim 3 \times 10^7$ s). But even for lab-scale classical promotion experiments, τ_p values in excess of 10^6 s are required (Fig. 14).

On the other hand, electrochemical promotion is not subject to any such restrictions regarding τ_p (Fig. 14). Thus when using O^{2-} conductors or H^+ conductors, t_p is 10^2–10^4 s, but when using Na^+ conductors τ_p can be well in excess of 10^7 s at low T, but also in the range 10^4–10^6 s for higher temperatures [16].

This is an important operational advantage of electrochemical promotion: It permits the use of a wide variety of sacrificial promoters (e.g., O^{2-}, H^+) which have life times too short for classical promotion applications.

3.5. Why the "new" supports

In view of the previous discussion the answer to the third question in Section 3.1 becomes obvious: For electrophobic reactions, i.e., for reactions which are accelerated via positive potential application in NEMCA experiments, or via supply of O^{2-} on the catalyst surface, the "new" supports, e.g., YSZ, CeO_2, doped TiO_2, are highly advantageous, since they offer continuous in situ promotion of the catalyst surface with backspillover O^{2-}, which is continuously replenished in the support by gaseous O_2. The catalyst support *acts as a catalyst for transforming gaseous O_2 to promoting O^{2-}, which continuously migrates on the catalyst surface*, where it weakens the chemisorptive bond energy of normally chemisorbed oxygen, thus accelerating the catalytic reaction.

Thus the frequently used "oxygen storage" mechanism [71] to interpret the beneficial properties of CeO_2 and of the other "new support" is, in a broad sense, correct. It is only the two distinct types of oxygen present on supported metal surfaces, one promoting, the other highly active, which is needed to complete the picture.

One can also appreciate why the above mechanism of metal–support interactions was extremely difficult to detect with surface spectroscopic techniques: The O^{2-} signal from the support can very effectively mask the O^{2-} signal from the dispersed catalyst surface. And if one uses $^{18}O_2$ as the gaseous oxidant, then only a fraction $f = 1/\Lambda$ of ^{16}O from the support will be found in the products. This fraction becomes significant only at elevated temperatures ($T >$ 550 °C), where Λ approaches unity and the phenomenon of electrochemical promotion with O^{2-} supports disappears [15,16], i.e., the double layer desorbs (Fig. 6b) and the limits of pure electrocatalysis are reached [15,16].

4. Double-layer approach to catalysis

4.1. Why double layer? Rationalization and prediction of desired types of promoters and supports

One of the major advances following the discovery of electrochemical promotion and the subsequent quest for understanding its molecular origin was the observation that the work function, Φ, of catalyst electrode surfaces changes with applied potential and, in fact, that over wide temperature and gas composition ranges (350–550 °C for YSZ, 200–420° for β''-Al_2O_3) the variation in Φ with catalyst potential U_{WR} is given by the following simple equation:

$$\Delta\Phi = e\Delta U_{WR}. \tag{6}$$

The ability to alter and control the work function of a catalyst surface via application of a potential caused strong interest among both leading surface scientists and electrochemists [58,84–86]. Eq. (6) is now established as a basic relationship in solid-state electrochemistry and together with [53]

$$\Phi_W - \Phi_R = eU_{WR} \tag{7}$$

allows for the definition of the absolute potential scale in solid-state electrochemistry [53]. Since the absolute potential of an electrode is a property of the support and of the gas composition, but not of the metal, the same concept can be used to define the absolute potential of a catalyst support [16,53]. This quantity, which equals Φ/e, where Φ is the work function of the support, plays an important role in quantifying the promotional aspects of catalyst supports used to induce metal–support interactions, as noted in Fig. 11.

The experimental Eqs. (6) and (7) suggest by themselves the double-layer approach to electrochemical promotion and, in view of the already discussed mechanistic equivalence of electrochemical promotion, promotion, and metal–support interactions [16], the double-layer approach to catalysis. The presence of an overall neutral double layer present at the metal/gas catalytic interface of catalysts is manifested simply by these equations, as follows [53].

In general, by definition [3,15,16] the equation

$$-\bar{\mu} = \Phi + e\Psi, \tag{8}$$

where $\bar{\mu}$ is the electrochemical potential (which always equals the Fermi level E_F of the metal [3,15,16]) and Ψ is

the outer or Volta potential, is valid for any metal catalyst or electrode.

Thus for a working (W) catalyst electrode and a reference (R) electrode one has

$$eU_{\mathrm{WR}} = \Phi_{\mathrm{W}} - \Phi_{\mathrm{R}} + e(\Psi_{\mathrm{W}} - \Psi_{\mathrm{R}}). \tag{9}$$

Comparison of the general theoretical Eq. (9) with the experimental Eqs. (6) and (7) gives

$$\Psi_{\mathrm{W}} - \Psi_{\mathrm{R}} = 0, \tag{10}$$

$$\Psi_{\mathrm{W}} = \Psi_{\mathrm{R}} = \text{constant}, \tag{11}$$

which in conjunction with Gauss's theorem of electrostatics gives for an overall neutral system $\Psi_{\mathrm{W}} = \Psi_{\mathrm{R}} = 0$ [53], i.e., the electrostatic Volta potential, Ψ, vanishes outside the double layer present at the catalyst/gas interface, because this double layer is, as is every double layer, overall neutral. Consequently one may conclude that promotion, electrochemical promotion, and metal–support interactions are all catalysis in the presence of a double layer. In the case of electrochemical promotion this double layer is in situ tunable via variation of the applied potential.

Thus one has the opportunity to study directly, at fixed temperature and gaseous composition, the effect of catalyst work function, Φ, on the kinetics of catalytic reactions.

4.2. The four types of rate–work function dependence and the promotional rules

As one would expect, four types of r vs Φ dependence are observed on varying the catalyst potential U_{WR} or work function Φ (Fig. 15).

1. Rate increase with potential and work function; i.e., $(\partial r/\partial\Phi)_{p_{\mathrm{A}},p_{\mathrm{D}}} > 0$, where p_{A} and p_{D} stand for the partial pressures of the electron acceptor (e.g., O_2, NO) and electron donor (e.g., C_2H_4, C_6H_6) reactant, respectively. These reactions are enhanced/suppressed when the catalyst–electrode is made positive/negative and thus have been termed electrophobic, from the words electron + phobos (fear). Practically all oxidations under fuel-lean conditions are electrophobic reactions [16, 87–89].
2. Rate decrease with work function; i.e. $(\partial r/\partial\Phi)_{p_{\mathrm{A}},p_{\mathrm{D}}} < 0$. Practically all oxidations under fuel-rich conditions and the reduction of NO by most hydrocarbons are electrophilic reactions [16,87].
3. Volcano-type reactions, where the rate passes through a maximum with varying work function. Typical examples are the oxidation of CO or H_2 on noble metals at low temperature [16,87].
4. Inverted volcano reactions, where the rate passes through a minimum with varying potential. Most catalytic reactions at elevated temperature exhibit inverted volcano behavior [16,87].

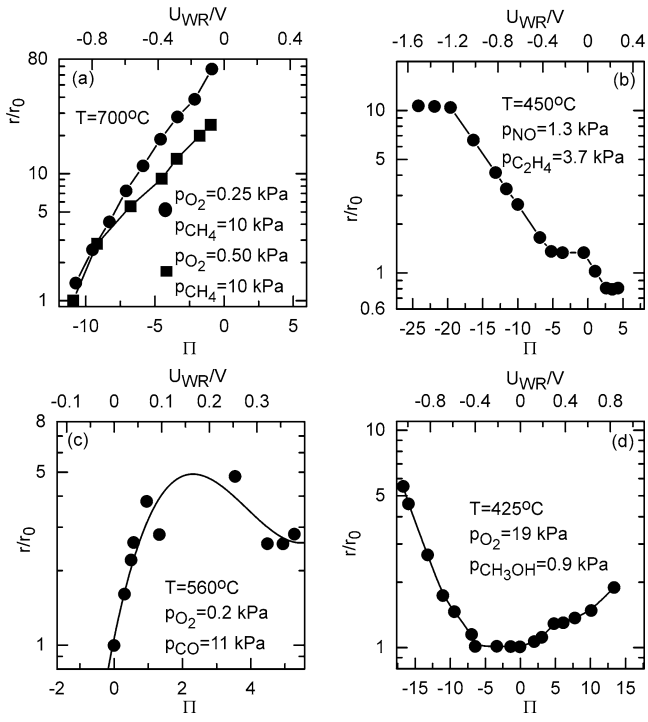

Fig. 15. Examples for the four types of global electrochemical promotion behavior: (a) electrophobic, (b) electrophilic, (c) volcano type, (d) inverted volcano type. (a) Effect of catalyst potential and work-function change (vs $I = 0$) for high (20 : 1 and 40 : 1) CH_4-to-O_2 feed ratios, Pt/YSZ. (b) Effect of catalyst potential on the rate enhancement ratio for the rate of NO reduction by C_2H_4 consumption on Pt/YSZ. (c) NEMCA-generated volcano plots during CO oxidation on Pt/YSZ. (d) Effect of dimensionless catalyst potential on the rate constant of H_2CO formation, Pt/YSZ ([87], and references therein). $\Pi = FU_{\mathrm{WR}}/RT\ (= \Delta\Phi/k_{\mathrm{b}}T)$.

In cases 1 and 2 the rate dependence on Φ is frequently found to satisfy the equation

$$\frac{r}{r_0} = \exp\left(\frac{\alpha\Delta\Phi}{k_{\mathrm{b}}T}\right), \tag{12}$$

where α is positive for electrophobic reactions and negative for electrophilic ones.

All classically or electrochemically promoted reactions can be grouped into these four categories [15,87]. Quite often, however, the same reaction changes its character, as one varies significantly the temperature or gaseous composition. Can one predict in which of the four categories a given catalytic reaction on a given metal belongs? Although electrophobic and electrophilic reactions have been known and studied since the 1980s [13,14] or even before, as the terms are synonymous to the terms electron acceptor and electron donor reaction, introduced by Wolkenstein in the 1960s [78], until very recently, a positive answer to the above basic question appeared to be a very distant goal. Yet, as shown very recently [87], there exist simple and rigorous rules which enable one to predict r vs Φ behavior. In simple terms a cat-

alytic reaction is

(i) *Electrophobic* if the electron acceptor is strongly bound on the catalyst surface and the electron donor is weakly bound,
(ii) *Electrophilic* if the opposite holds, i.e., if the electron acceptor is weakly bound and the electron donor is strongly bound,
(iii) *Volcanotype* if both reactants are strongly bound on the catalyst surface, and
(iv) *Inverted volcanotype* if both reactants are weakly bound on the catalyst surface.

Conversely, if a reaction is electrophobic one can predict that the kinetics are positive order in D and zero or negative order in A. If a reaction is electrophilic, one can predict that its kinetics are negative or zero order in D and positive order in A. If a reaction is a volcano type, then the rate vs both p_D and p_A passes through a maximum. And if a reaction is inverted volcano, then the kinetics are positive order in both A and D [87].

These rules appear to have no exceptions [87–89]. They have been derived on the basis of more than 70 electrochemical and classical promotion studies [16,87], and we have recently shown that there have been no exceptions to these rules in the last 10 years of the *Journal of Catalysis* [90].

In mathematical terms, rules 1 to 3 can be expressed as [87]

$$\left(\frac{\partial r}{\partial \Phi}\right)_{p_A,p_D}\left(\frac{\partial r}{\partial p_D}\right)_{\Phi,p_A} > 0; \tag{13}$$

i.e., the r vs Φ dependence traces (has the same sign with) the r vs p_D dependence. Conversely, since in the presence of a double layer at the metal/gas interface it is $\Phi = -E_F$, the above equation can be written as

$$\left(\frac{\partial r}{\partial E_F}\right)_{p_A,p_D}\left(\frac{\partial r}{\partial p_A}\right)_{E_F,p_D} > 0; \tag{14}$$

i.e., the r vs catalyst Fermi level dependence traces (has the same sign with) the rate vs p_A dependence.

The above rules 1 to 4 stem [87] from the two fundamental rules

$$\left(\frac{\partial \theta_D}{\partial \Phi}\right)_{p_A,p_D} \geqslant 0, \tag{15}$$

$$\left(\frac{\partial \theta_A}{\partial \Phi}\right)_{p_A,p_D} \leqslant 0, \tag{16}$$

which express the fact that increasing catalyst work function enhances the chemisorptive bond strength of electron donor adsorbates and weakens the chemisorptive bond strength of electron acceptor adsorbates. Both "fundamental" rules are in good agreement with the experimentally observed variation of adsorption enthalpies, ΔH_j, with work function [16,87]; i.e.,

$$\Delta|\Delta H_j| = \alpha_{H,j}\Delta\Phi, \tag{17}$$

where $\alpha_{H,j} > 0$ for electron donor adsorbates, and $\alpha_{H,j} < 0$ for electron acceptor adsorbates. Eq. (17) is also in excellent agreement with rigorous quantum mechanical calculations [56,57].

The above four rules enable one to derive the following three "practical" rules [87] for promoter selection:

1. If a catalyst surface is predominantly covered by an electron acceptor reactant, e.g., O, then an electron acceptor promoter, e.g., O^{2-}, is to be recommended.
2. If a catalyst surface is covered predominantly by an electron donor reactant (e.g., C_6H_6, C_2H_4), then an electron donor promoter (e.g., Na^+, Ka^+) is to be recommended.
3. If both reactants are weakly adsorbed on the catalyst surface, then both electron acceptor and electron donor additives can enhance the rate.

Clearly all the above rules are valid as long as site blocking by the promoter does not become a dominant factor [16].

Regarding metal–support interactions involving O^{2-}-conducting oxides, the following rule can be derived: *Metal–support interactions with oxidic ion conducting or mixed ionic–electronic conducting supports can enhance the rate of a catalytic reaction only when the reaction is electrophobic.*

An example is shown in Fig. 11 for the case of C_2H_4 oxidation on Rh supported on various supports of increasing absolute potential and work function.

4.3. Double-layer isotherms and kinetics

The experimentally proven existence of an overall neutral effective double layer at the metal/gas interface has been utilized recently [88,89] to derive, starting from simple and rigorous thermodynamic and electrostatic principles, adsorption isotherms which account explicitly for the electrostatic interactions between the adsorbates and the double layer (Fig. 8).

One starts from the equilibrium adsorption condition,

$$\bar{\mu}_j(g) = \bar{\mu}_j(ad) = \mu_j(ad) + \widetilde{P}_j \cdot \widetilde{E} \cdot N_{AV}, \tag{18}$$

where $\bar{\mu}_j$ is the electrochemical potential of adsorbed species j, μ_j is its chemical potential, $\widetilde{P}_j$, taken as a vector is its dipole moment in the adsorbed state, $\widetilde{E}$ is the local field strength in the double layer, assumed uniform, and N_{AV} is Avogadro's constant.

The equilibrium condition leads to the effective double-layer (EDL) isotherm

$$k_j p_j = \big(\theta_j/(1-\theta_j)\big)\exp(-\lambda_j \Pi), \tag{19}$$

with

$$\Pi = \Delta\Phi\left(\frac{\ell}{2d}\cos\omega\right)\Big/ k_b T, \tag{20}$$

$$k_j = \exp\big(\big(\mu_j^o(g) - \mu_j^o(ad)\big)/RT\big), \tag{21}$$

where $\Delta\Phi$ is the deviation of the work function, Φ, from its value at the potential of zero charge (pzc) of the double layer, ℓ is the dipole length, d is the double-layer thickness (Fig. 8), ω is the angle formed between the adsorbate dipole and the field strength, and λ_j is the partial charge transfer parameter. This parameter is zero for a truly covalent chemisorptive bond, positive for an electron donor adsorbate and negative for an electron acceptor adsorbate.

Using Eq. (18) with $\cos\omega = 1$ and the definition of the isosteric enthalpy of adsorption $H_{\rm ad} = T^2(\partial(\bar{\mu}_{j\,({\rm ad})})/T)_{p_j,\theta_j}$, one can derive that

$$\Delta H_{{\rm ad},j} = \Delta H^{\rm o}_{{\rm ad},j} + \frac{\lambda_j \ell}{2d}\Delta\Phi, \tag{22}$$

where $\Delta H^{\rm o}_{{\rm ad},j}$ is the heat of adsorption for $\Delta\Phi = 0$. Assuming $\ell \approx d$, one obtains

$$\Delta H_{{\rm ad},j} = \Delta H^{\rm o}_{{\rm ad},j} + (\lambda_j/2)\Delta\Phi. \tag{23}$$

Thus for an electron acceptor adsorbate ($\lambda_j < 0$), Eqs. (22) and (23) predict a linear decrease in $\Delta H_{\rm ad}$ with increasing $\Delta\Phi$, while for electron donor adsorbates ($\lambda_j > 0$) they predict a linear decrease in $\Delta H_{\rm ad}$ with decreasing $\Delta\Phi$. Both predictions are in excellent agreement with experiment (Eq. (17)) [16,87] and with rigorous quantum mechanical calculations [56,57].

One can use the effective double-layer isotherm (Eq. (21)) to derive analytical mathematic expressions for catalytic promotional kinetics [88]. For the case of surface reaction rate control the corresponding expression is

$$r = \frac{k_{\rm R}k_{\rm A}k_{\rm D}p_{\rm A}p_{\rm D}\exp[(\lambda_{\rm D}+\lambda_{\rm A})\Pi]}{[1+k_{\rm D}p_{\rm D}\exp(\lambda_{\rm D}\Pi)+k_{\rm A}p_{\rm A}\exp(\lambda_{\rm A}\Pi)]^2}, \tag{24}$$

where $k_{\rm R} = k^{\rm o}_{\rm R}\exp(\lambda_{\rm R}\Pi)$ and $\lambda_{\rm R}$ is the partial charge transfer parameter of the transition state.

In the limit of very weak adsorption ($k_{\rm A}p_{\rm A}, k_{\rm D}p_{\rm D} \ll 1$) one may neglect repulsive interactions [87,88] and consider only the attractive ones. In this case Eq. (24) becomes

$$r = k_{\rm R}k_{\rm D}k_{\rm A}p_{\rm D}p_{\rm A}\exp\big[\max(0,\lambda_{\rm D}\Pi)+\max(0,\lambda_{\rm A}\Pi)\big] \Big/ \Big(1+k_{\rm D}p_{\rm D}\exp\big[\max(0,\lambda_{\rm D}\Pi)\big] + k_{\rm A}p_{\rm A}\exp\big[\max(0,\lambda_{\rm A}\Pi)\big]\Big)^2, \tag{25}$$

where $\max(x, y)$ denotes x and $x > y$, y when $x < y$, and x or y when $x = y$.

The success of Eqs. (24) and (25) in describing the above recently derived promotional rules can be appreciated from Fig. 16, which shows the transition from electrophobic to electrophilic to volcano-type and to inverted volcano-type behavior by simply varying the values of the adsorption equilibrium constants $k_{\rm D}$ and $k_{\rm A}$.

Also the success of double-layer kinetics can also be appreciated from Fig. 17, which compares model predictions (Figs. 17a and 17b) with some interesting and complex experimental results (Figs. 17c and 17d) obtained during C_2H_4 oxidation on Pt/TiO_2 [39,88]. As shown in Figs. 17c and 17d

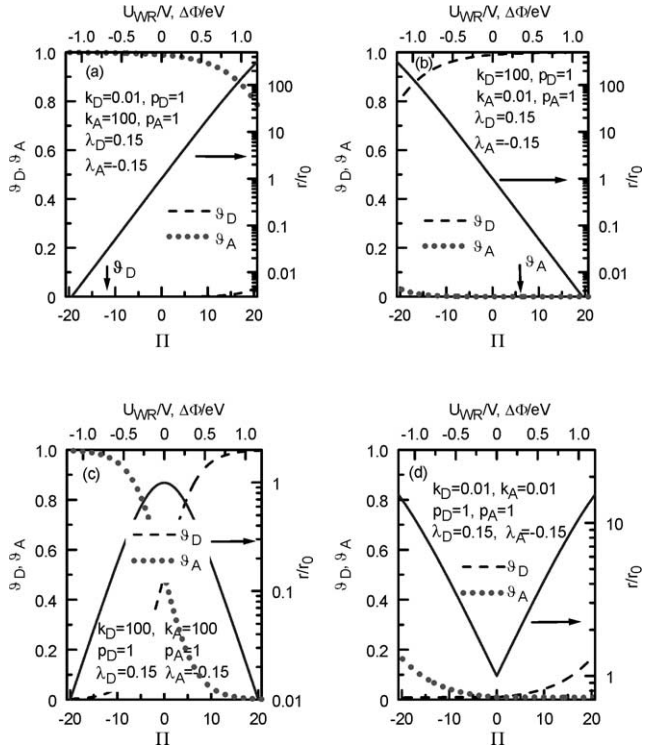

Fig. 16. Effective double-layer model-predicted electrochemical or classical promotion behavior: (a) electrophobic, (b) electrophilic, (c) volcano type, (d) inverted volcano type [88].

the rate dependence on $U_{\rm WR}$ and Π shifts from inverted volcano (Fig. 17c) to purely electrophobic (Fig. 17d) as $p_{C_2H_4}$ ($= p_{\rm D}$) is decreased by a factor of 10 at fixed p_{O_2}.

As shown in Figs. 17a and 17b the model predicts the shift in global behavior in a semiquantitative manner and in fact with very reasonable $\lambda_{\rm D}$ and $\lambda_{\rm A}$ values ($\lambda_{\rm D} > 0$, $\lambda_{\rm A} < 0$).

Finally the success of the model can be judged from Figs. 18a and 18b, which show the experimental and model-predicted rate dependence on $p_{\rm CO}$ and work function during CO oxidation on Pt/β''-Al_2O_3 [37,88]. Note the transition from a classical Langmuir–Hinshelwood to a positive-order rate dependence on $p_{\rm CO}$ with decreasing work function. Also notice that on every point of the experimental or model-predicted rate dependence, the basic promotional rule, Eq. (13) is strictly obeyed. The optimal $\lambda_{\rm D}$ and $\lambda_{\rm A}$ values are again quite reasonable ($\lambda_{\rm D} > 0$, $\lambda_{\rm A} < 0$). The large optimal $k_{\rm A}$ and $k_{\rm D}$ values (~ 9) are also quite reasonable, as they indicate strong adsorption of both CO ($=$ D) and oxygen ($=$ A), which is the necessary and sufficient condition (rule 3) for the appearance of volcano-type behavior.

In general Figs. 16–18 show, beyond any reasonable doubt, that the effective double-layer model of promotion, expressed mathematically by Eqs. (24) and (25), provides a satisfactory description of promotional kinetics.

Despite the very good success of the effective double-layer model, it is useful to remember that as an effective-

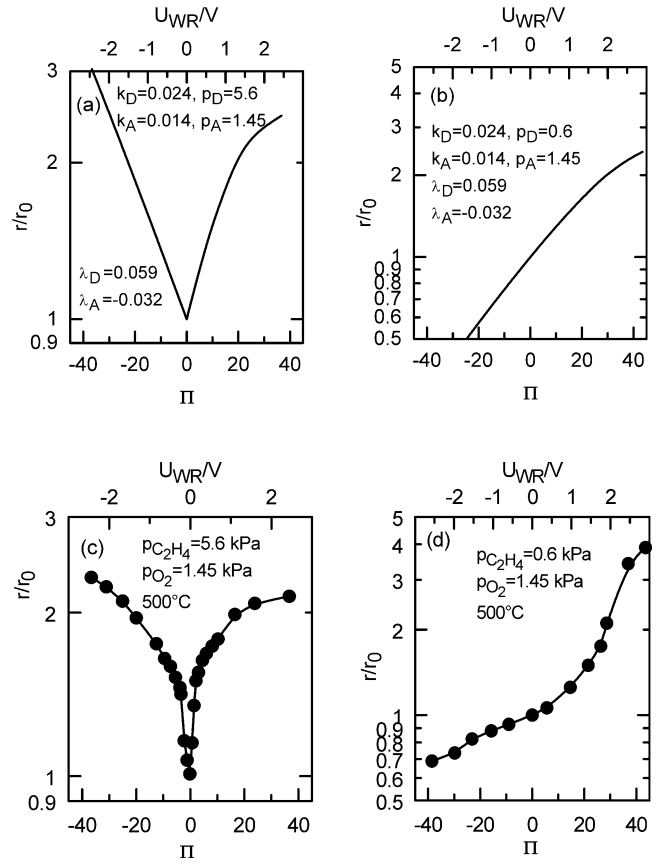

Fig. 17. Experimentally observed [39] (bottom) and model predicted (top) transition from inverted volcano to electrophobic behavior on increasing the O_2 to ethylene (i.e., A/D) ratio by a factor of 10; C_2H_4 oxidation on Pt/TiO_2 [88].

medium model, it cannot be expected to describe local geometric or surface ensemble effects. We can consider as an example the case of Cu addition on polycrystalline Ru surfaces used for hydrogenolysis/hydrogenation reactions. While the effect of Cu on the chemisorption of hydrogen on Ru can be reasonably expected to be described by the double-layer model, the decoration of steps and defects of Ru by Cu, which blocks hydrogenolysis but does not affect hydrogenation, is almost certainly not a double-layer effect.

The usefulness of the effective double layer isotherm (Eq. (19)) is not limited to the description of promotional kinetics. As discussed elsewhere [16,90], it can also be used to derive the Nernst equation but also the Butler–Volmer equation. The former is the basic equilibrium equation in electrochemistry and the latter is the basic kinetic equation in electrochemistry and electrocatalysis [3,4]. Thus both promotional catalytic and electrocatalytic kinetics can be modeled using the same type of isotherm [88]. This is because both electrocatalysis and catalysis on metals can be viewed as chemical reaction between dipoles in presence of a double layer.

5. Summary and perspectives

The search for understanding the phenomenon of electrochemical promotion at the molecular level during the last 10 years, by utilizing a wide variety of surface science and electrochemical techniques, has not only accomplished its initial goal, it perhaps more important, has been particularly fruitful in defining, tackling, and solving to a satisfactory degree several additional important problems in heterogeneous catalysis. This was partly due to the unique ability offered by electrochemical promotion to allow for in situ examination of the effect of promoters and of catalyst work function on catalytic activity and selectivity. Thus during the last 5 years the following compelling evidence has been obtained.

1. Electrochemical promotion is functionally identical to classical promotion; i.e., it is catalysis in the presence of a controllable double layer at the metal/gas interface. The main advantage of electrochemical promotion is that it also allows the use of short-lived *sacrificial* promoters, such as O^{2-}, which are continuously supplied to the catalyst/gas interface via electrochemically

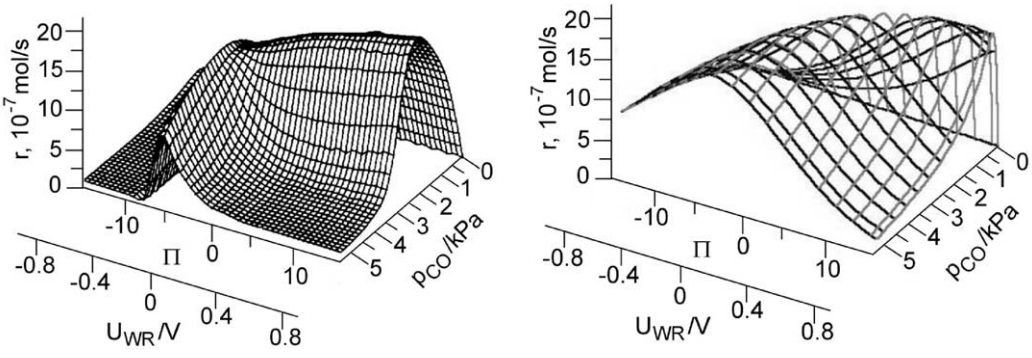

Fig. 18. Experimental [37] (left) and model simulated [88] (right) dependence of the rate of CO oxidation on Pt deposited on β''-Al_2O_3 as a function of p_{CO}, catalyst potential U_{WR}, and dimensionless catalyst work function Π ($= \Delta\Phi/k_bT$) at $p_{O_2} = 6$ kPa. Parameters used in Eq. (24): $k_A = 9.133$, $k_D = 8.715$, $\lambda_A = -0.08$, $\lambda_D = 0.09$, $\lambda_R = 0$, $k_R = 6.19 \times 10^{-6}$ mol/s.

controlled reverse spillover from the solid electrolyte support.

2. Metal–support interactions of ZrO_2-, CeO_2-, Y_2O_3-, and TiO_2-based supports are due to a self-driven electrochemical promotional mechanism, i.e., continuous migration of sacrificial promoter O^{2-} from the support to the metal/gas interface and continuous replenishment of O^{2-} in the support from gaseous O_2. Electrochemical promotion itself is an electrically controlled metal–support interaction. Metal–support interactions with these supports can only promote electrophobic reactions.
3. Depending on their r vs Φ dependence, catalytic reactions are grouped into four categories: electrophobic, electrophilic, volcano, and inverted volcano. Rigorous rules have been derived which enable one to predict in which category a given catalytic reaction belongs, on the basis of its unpromoted kinetics. The same rules also enable one to predict the kinetics with respect to the electron acceptor or donor reactants (positive, zero, or negative order) when the r vs Φ dependence is known.
4. The absolute potential of ionic or mixed ionic–electronic conducting supports has been defined and measured. It equals Φ^o/e, where Φ^o is the work function of the support under selected standard conditions.
5. For electrophobic reactions, electronegative promoters and high-work-function supports enhance significantly the catalytic activity.
6. For electrophilic reactions, electropositive promoters and low-work-function supports enhance significantly the catalytic activity.
7. Electrochemical promotion, classical promotion, and also metal–support interactions [16] can be modeled, similarly to electrocatalysis [16], by using simple and rigorous double-layer isotherms which utilize the fact that promotion, electrochemical promotion, and metal–support interactions are different facets of the same phenomenon, i.e., catalytic reaction in the presence of a double layer, which for the case of electrochemical promotion is in situ controllable [88].

Thus, aside from the very likely forthcoming technological applications [16,41,91], electrochemical promotion is a unique and efficient tool for studying the heart of classical catalysis, namely promotion and metal–support interactions.

Although electrochemical promotion of dispersed catalysts has been already reported for some catalysts supported on carbon [38,92], Au [93], and CeO_2–Gd_2O_3 [41], one of the main future challenges will be to extend these studies to finely dispersed catalysts on ZrO_2, TiO_2, or novel proton conducting supports [94–96], some of which [94,95] can operate in the temperature range 100–300 °C. This could create several new opportunities in selective hydrogenation and isomerization [95] and in the production of fine chemicals.

Acknowledgments

We thank BASF and the EU Growth and TMR programmes for financial support and our reviewers for their thoughtful comments.

References

[1] L.L. Hegedus, R. Aris, A.T. Bell, M. Boudart, N.Y. Chen, B.C. Gates, W.O. Haag, G.A. Somorjai, J. Wei, Catalyst Design: Progress and Perspectives, Wiley, New York, 1987.
[2] G. Ertl, H. Knötzinger, J. Weitcamp, Handbook of Catalysis, VCH, Weinheim, 1997.
[3] J.O.M. Bockris, A.K.M. Reddy, M. Gamboa-Aldeco, Modern Electrochemistry, No. 2A, 2B, Kluwer Academic/Plenum, New York, 2000.
[4] C.H. Hamann, A. Hamnett, W. Vielstich, Electrochemistry, Wiley–VCH, Weinheim, 1998.
[5] G.A. Somorjai, Chemistry in Two Dimensions: Surfaces, Cornell Univ. Press, Ithaca, NY, 1981.
[6] T. Engel, G. Ertl, in: D.A. King, D.P. Woodruff (Eds.), Chemical Physics of Solid Surfaces and Heterogeneous Catalysis, Vol. 4, 1982.
[7] A. Wieckowski, Interfacial Electrochemistry, Theory, Experiments and Applications, Dekker, New York, 2000.
[8] A. Wieckowski, E. Savinova, C.G. Vayenas, Catalysis and Electrocatalysis at Nanoparticles, Dekker, New York, in press.
[9] S.C. Singhal, Solid State Ionics 135 (2000) 305.
[10] F.R. Kalhammer, Solid State Ionics 135 (2000) 315.
[11] P. Wasczuk, A. Wieckowski, P. Zelenay, S. Gottesfeld, C. Contanceau, J.-M. Leger, C. Lamy, J. Electroanal. Chem. 511 (2001) 55.
[12] M. Stoukides, C.G. Vayenas, J. Catal. 70 (1981) 137.
[13] C.G. Vayenas, S. Bebelis, S. Neophytides, J. Phys. Chem. 92 (1988) 5083.
[14] C.G. Vayenas, S. Bebelis, S. Ladas, Nature 343 (1990) 625.
[15] C.G. Vayenas, M.M. Jaksic, S. Bebelis, S.G. Neophytides, in: J.O.M. Bockris, B.E. Conway, R.E. White (Eds.), The Electrochemical Activation of Catalysis, Vol. 29, Kluwer Academic/Plenum, New York, 1996, p. 57.
[16] C.G. Vayenas, S. Bebelis, C. Pliangos, S. Brosda, D. Tsiplakides, Electrochemical Activation of Catalysis: Promotion, Electrochemical Promotion and Metal-Support Interactions, Kluwer Academic/Plenum, New York, 2001.
[17] R.M. Lambert, F. Williams, A. Palermo, M.S. Tikhov, Top. Catal. 13 (2000) 91.
[18] C. Wagner, Adv. Catal. 21 (1970) 323.
[19] C.G. Vayenas, H.M. Saltsburg, J. Catal. 57 (1979) 296.
[20] G. Foti, S. Wodiunig, C. Comninellis, Curr. Top. Electrochem. 7 (2001) 1.
[21] T.I. Politova, V.A. Sobyanin, V.D. Belyaev, React. Kinet. Catal. Lett. 41 (2) (1990) 321.
[22] O.A. Mar'ina, V.A. Sobyanin, Catal. Lett. 13 (1992) 61.
[23] E. Varkaraki, J. Nicole, E. Plattner, C. Comninellis, C.G. Vayenas, J. Appl. Electrochem. 25 (1995) 978.
[24] I. Harkness, R.M. Lambert, J. Catal. 152 (1995) 211.
[25] I.R. Harkness, C. Hardacre, R.M. Lambert, I.V. Yentekakis, C.G. Vayenas, J. Catal. 160 (1996) 19.
[26] C. Cavalca, G. Larsen, C.G. Vayenas, G. Haller, J. Phys. Chem. 97 (1993) 6115.
[27] C.A. Cavalca, G.L. Haller, J. Catal. 177 (1998) 389.
[28] H. Baltruschat, N.A. Anastasijevic, M. Beltowska-Brzezinska, G. Hambitzer, J. Heitbaum, Ber. Bunsenges. Phys. Chem. 94 (1990) 996.
[29] L. Ploense, M. Salazar, B. Gurau, E.S. Smotkin, J. Am. Chem. Soc. 119 (1997) 11550.
[30] J. Poppe, S. Voelkening, A. Schaak, E. Schuetz, J. Janek, R. Imbihl, Phys. Chem. Chem. Phys. 1 (1999) 5241.

[31] I.M. Petrushina, V.A. Bandur, F. Cappeln, N.J. Bjerrum, J. Electrochem. Soc. 147 (8) (2000) 3010.
[32] J.K. Hong, I.-H. Oh, S.-A. Hong, W.Y. Lee, J. Catal. 163 (1996) 95.
[33] E. Lamy-Pitara, S.E. Mouahid, J. Barbier, Electrochim. Acta 45 (2000) 4299.
[34] P. Vernoux, F. Gaillard, L. Bultel, E. Siebert, M. Primet, J. Catal. 208 (2002) 412.
[35] S. Bebelis, C.G. Vayenas, J. Catal. 118 (1989) 125.
[36] M. Makri, A. Buekenhoudt, J. Luyten, C.G. Vayenas, Ionics 2 (1996) 282.
[37] I.V. Yentekakis, G. Moggridge, C.G. Vayenas, R.M. Lambert, J. Catal. 146 (1994) 292.
[38] S. Neophytides, D. Tsiplakides, P. Stonehart, M. Jaksic, C.G. Vayenas, Nature 370 (1994) 292.
[39] C. Pliangos, I.V. Yentekakis, S. Ladas, C.G. Vayenas, J. Catal. 159 (1996) 189.
[40] P.D. Petrolekas, S. Balomenou, C.G. Vayenas, J. Electrochem. Soc. 145 (4) (1998) 1202.
[41] H. Christensen, J. Dinesen, H.H. Engell, L.C. Larsen, K.K. Hansen, E.M. Skou, Electrochemical exhaust gas purification, SAE paper 2000-01-0478, Diesel Exhaust Aftertreatment 2000 (SP 1497), 141–145, 2000.
[42] C.G. Vayenas, S. Bebelis, I.V. Yentekakis, H.-G. Lintz, Catal. Today 11 (3) (1992) 1.
[43] T. Hibino, S. Wang, S. Kakimoto, M. Sano, Solid State Ionics 127 (2000) 89.
[44] T. Arakawa, A. Saito, J. Shiokawa, Appl. Surf. Sci. 16 (1983) 365.
[45] S. Ladas, S. Kennou, S. Bebelis, C.G. Vayenas, J. Phys. Chem. 97 (1993) 8845.
[46] W. Zipprich, H.-D. Wiemhöfer, U. Vöhrer, W. Göpel, Ber. Bunsen-Ges. Phys. Chem. 99 (1995) 1406.
[47] S.G. Neophytides, C.G. Vayenas, J. Phys. Chem. 99 (1995) 17063.
[48] D. Tsiplakides, C.G. Vayenas, J. Catal. 185 (1999) 237.
[49] S. Neophytides, D. Tsiplakides, C.G. Vayenas, J. Catal. 178 (1998) 414.
[50] D. Tsiplakides, S. Neophytides, C.G. Vayenas, Solid State Ionics 136–137 (2000) 839.
[51] J. Poppe, A. Schaak, J. Janek, R. Imbihl, Ber. Bunsenges. Phys. Chem. 102 (1998) 1019.
[52] M. Makri, C.G. Vayenas, S. Bebelis, K.H. Besocke, C. Cavalca, Surf. Sci. 369 (1996) 351.
[53] D. Tsiplakides, C.G. Vayenas, J. Electrochem. Soc. 148 (5) (2001) E189.
[54] D. Kek, M. Mogensen, S. Pejovnik, J. Electrochem. Soc. 148 (8) (2001) A878.
[55] A.D. Frantzis, S. Bebelis, C.G. Vayenas, Solid State Ionics 136–137 (2000) 863.
[56] G. Pacchioni, F. Illas, S. Neophytides, C.G. Vayenas, J. Phys. Chem. 100 (1996) 16653.
[57] G. Pacchioni, J.R. Lomas, F. Illas, Mol. Catal. A 119 (1997) 263.
[58] J. Pritchard, Nature 343 (1990) 592.
[59] J. Nicole, C. Comninellis, J. Appl. Electrochem. 28 (1998) 223.
[60] J.-F. Lambert, M. Che, J. Mol. Catal. A 162 (2000) 5.
[61] B.N. Shelimov, J.-F. Lambert, M. Che, B. Didillon, J. Mol. Catal. A 158 (2000) 91.
[62] I.M. Campbell, Catalysis at Surfaces, Chapman & Hall, London/New York, 1988.
[63] M. Kiskinova, in: Poisoning and Promotion in Catalysis Based on Surface Science Concepts and Experiments, Vol. 70, Elsevier, Amsterdam, 1992.
[64] G.-M. Schwab, Adv. Catal. 27 (1978) 1.
[65] F. Solymosi, Catal. Rev.–Sci. Eng. 1 (1967) 233.
[66] S.J. Tauster, S.C. Fung, R.L. Garten, J. Am. Chem. Soc. 100 (1978) 170.
[67] G.L. Haller, D.E. Resasco, Adv. Catal. 36 (1989) 173.
[68] E.C. Akubuiro, X.E. Verykios, J. Catal. 113 (1988) 106.
[69] M. Haruta, A. Ueda, S. Tsubota, R.M.T. Sanchez, Catal. Today 29 (1996) 443.
[70] B.L. Mojet, J.T. Miller, D.E. Ramaker, D.C. Koningsberger, J. Catal. 186 (1999) 373.
[71] R.J. Farrauto, C.H. Bartholomew, Fundamentals of Industrial Catalytic Processes, Chapman & Hall, London, 1997.
[72] Z. Hong, K.B. Fogash, J.A. Dumesic, Catal. Today 51 (1999) 269.
[73] D.G. Barton, M. Shtein, R.D. Wilson, S.L. Soled, E. Iglesia, J. Phys. Chem. 103 (4) (1999) 630.
[74] G. Meitzner, E. Iglesia, Catal. Today 53 (1999) 433.
[75] S. Tagliaferri, R.A. Koeppel, A. Baiker, Appl. Catal. B 15 (1998) 159.
[76] A.Y. Stakheev, L.M. Kustov, Appl. Catal. A 188 (1999) 3.
[77] A. Cimino, D. Gazzoli, M. Valigi, J. Electron Spectrosc. Relat. Phenom. 104 (1999) 1.
[78] T. Wolkenstein, Elektronentheorie der Katalyse an Halbleitern, VEB, Berlin, 1964.
[79] D. Tsiplakides, D. Archonta, C.G. Vayenas, submitted for publication.
[80] J. Nicole, D. Tsiplakides, C. Pliangos, X.E. Verykios, C. Comninellis, C.G. Vayenas, J. Catal. 204 (2001) 23.
[81] C.A. Pliangos, I.V. Yentekakis, V.G. Papadakis, C.G. Vayenas, X.E. Verykios, Appl. Catal. B 14 (1997) 161.
[82] J. Nicole, PhD thesis, EPFL, Lausanne, 1999.
[83] C.G. Vayenas, G. Pitselis, Ind. Eng. Chem. Res. 40 (20) (2001) 4209.
[84] J.O.M. Bockris, Z.S. Minevski, Electrochim. Acta 39 (11/12) (1994) 1471.
[85] G.-Q. Lu, A. Wieckowski, Curr. Opin. Colloid Interface Sci. 5 (2000) 95.
[86] B. Grzybowska-Swierkosz, J. Haber, in: Annual Reports on the Progress of Chemistry, Vol. 91, Royal Soc. Chemistry, Cambridge, 1994, p. 395.
[87] C.G. Vayenas, S. Brosda, C. Pliangos, J. Catal. 203 (2001) 329.
[88] S. Brosda, C.G. Vayenas, J. Catal. 208 (2002) 38.
[89] C.G. Vayenas, S. Brosda, Stud. Surf. Sci. Catal. 138 (2001) 197.
[90] C.G. Vayenas, S. Brosda, manuscript in preparation.
[91] S. Wodiunig, F. Bokeloh, J. Nicole, C. Comninellis, Electrochem. Solid State Lett. 2 (6) (1999) 281.
[92] S. Neophytides, D. Tsiplakides, P. Stonehart, M.M. Jaksic, C.G. Vayenas, J. Phys. Chem. 100 (1996) 14803.
[93] M. Marwood, C.G. Vayenas, J. Catal. 178 (1998) 429.
[94] I.M. Petrushina, V.A. Bandur, N.J. Bjerrum, F. Cappeln, L. Qingfeng, J. Electrochem. Soc. 149 (2002) D143.
[95] L. Ploense, M. Salazar, B. Gurau, E. Smotkin, Solid State Ionics 136–137 (2000) 713.
[96] C.G. Yiokari, G.E. Pitselis, D.G. Polydoros, A.D. Katsaounis, C.G. Vayenas, J. Phys. Chem. 104 (2000) 10600.